

## Supporting Information for

# Prolonging the Lifetime of Ultralong Organic Phosphorescence through Dihydrogen Bonding

Long Gu,<sup>‡[a](#)</sup> Huifang Shi,<sup>‡[a](#)</sup> Chunyang Miao,<sup>a</sup> Qi Wu,<sup>a</sup> Zhichao Cheng,<sup>a</sup> Suzhi Cai,<sup>a</sup> Mingxing Gu,<sup>a</sup> Chaoqun Ma,<sup>a</sup> Wei Yao,<sup>a</sup> Yaru Gao,<sup>a</sup> Zhongfu An,<sup>\*[a](#)</sup> Wei Huang<sup>\*[a b](#)</sup>

<sup>a</sup>Key Laboratory of Flexible Electronics (KLOFE) & Institute of Advanced Materials (IAM), Jiangsu National Synergetic Innovation Center for Advanced Materials (SICAM), Nanjing Tech University (NanjingTech), 30 South Puzhu Road, Nanjing, 211816, P.R. China. E-mail:  
iamzfan@njtech.edu.cn; iamwhuang@njtech.edu.cn

<sup>b</sup>Shaanxi Institute of Flexible Electronics (SIFE), Northwestern Polytechnical University (NPU), 127 West Youyi Road, Xi'an 710072, China.

## **Table of Contents**

**I. Experimental section**

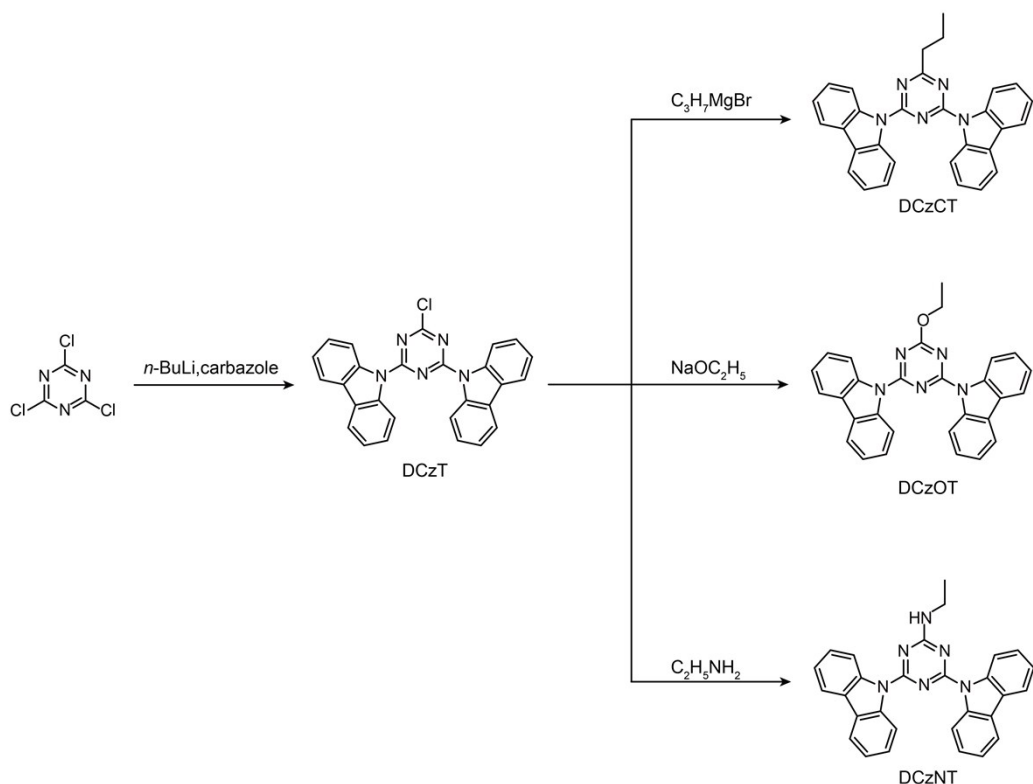
**II. Additional photophysical properties of organic phosphors in solution and crystal state**

**III. Theoretical calculations**

**IV. Single crystal data**

**V. Complementary videos**

## Experimental Section



**Scheme S1.** Synthetic routes of DCzCT, DCzOT and DCzNT.

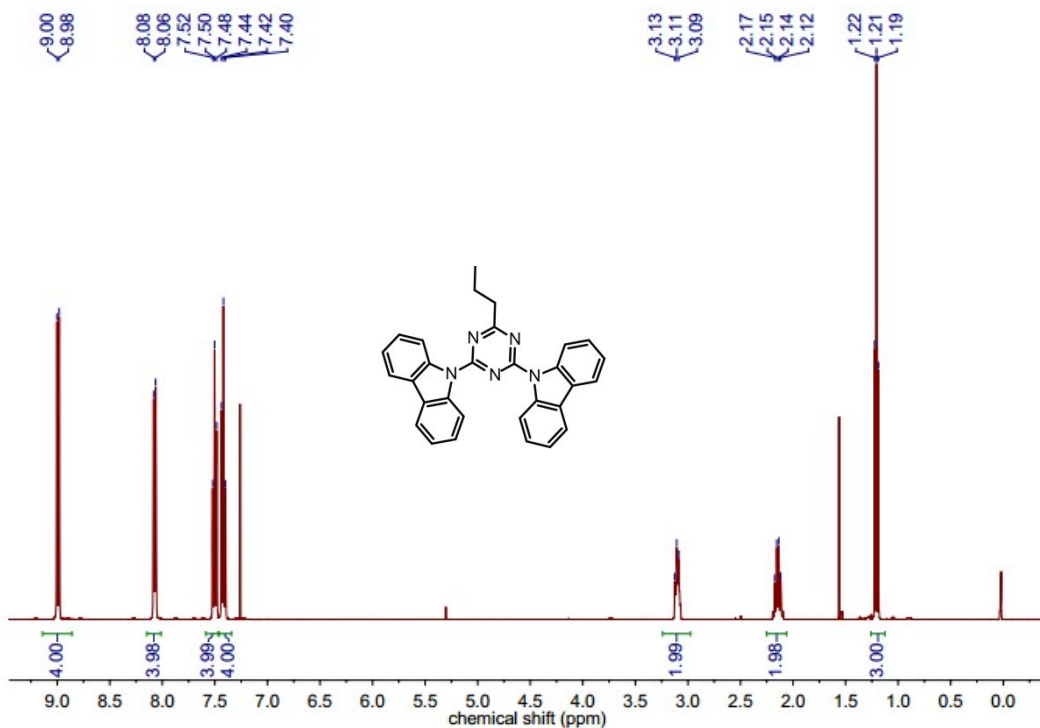


**Figure S1.**  $^1\text{H}$  NMR spectrum of DCzCT in  $\text{CDCl}_3$ .

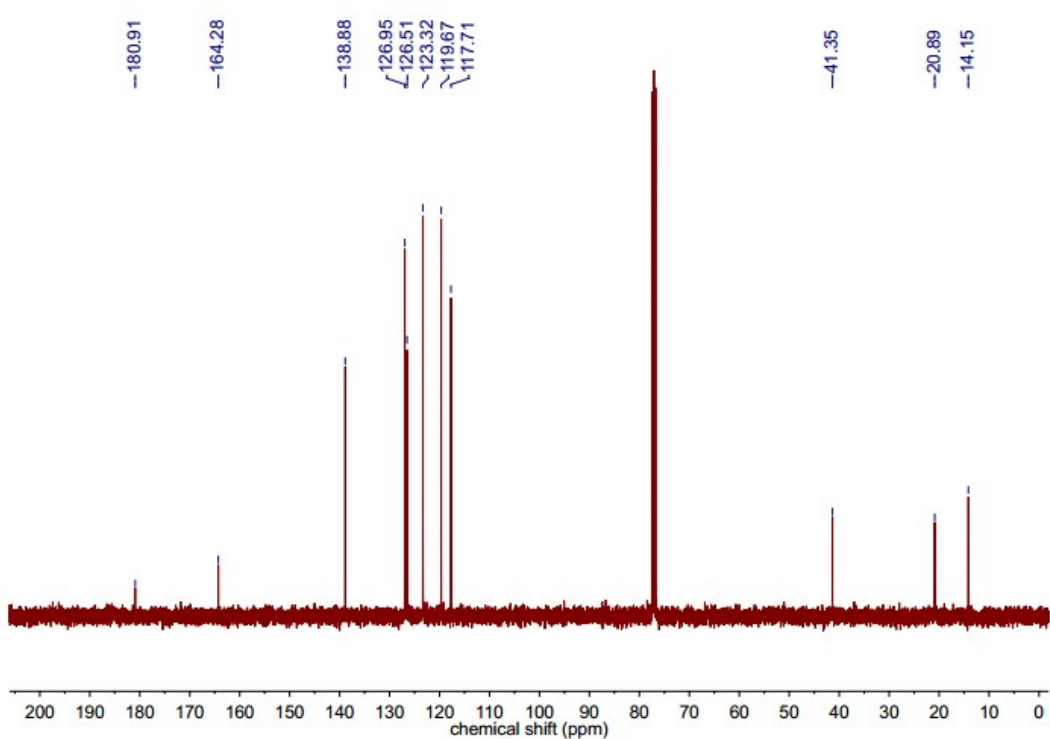


**Figure S2.**  $^{13}\text{C}$  NMR spectrum of DCzCT in  $\text{CDCl}_3$ .

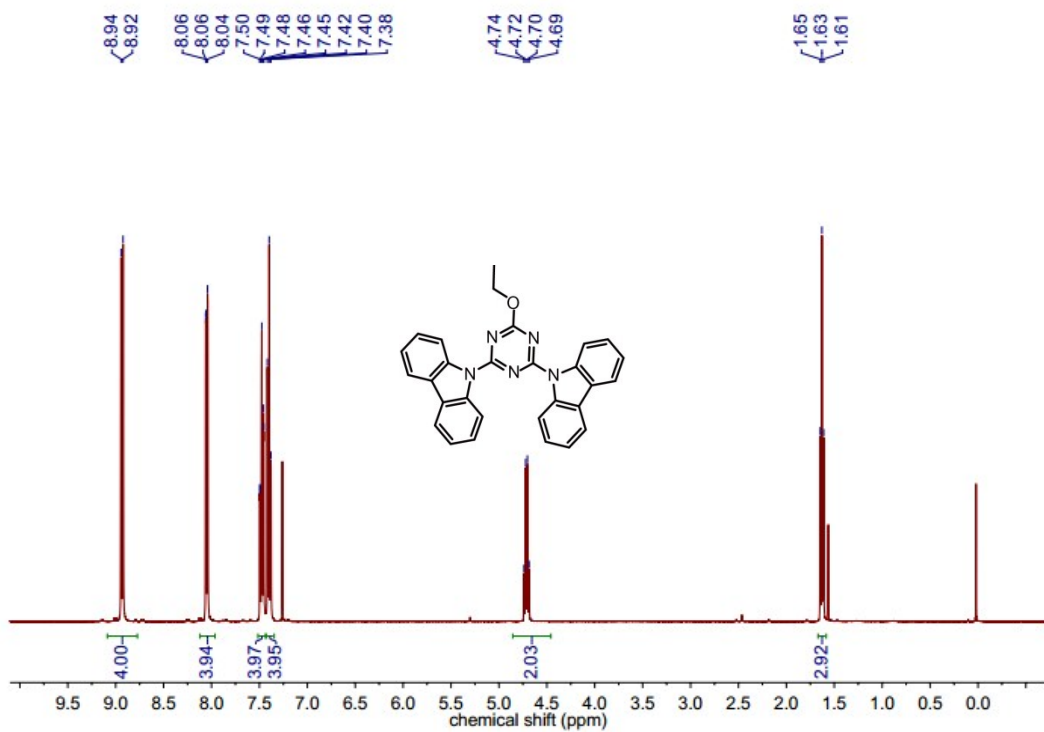


**Figure S3.**  $^1\text{H}$  NMR spectrum of DCzOT in  $\text{CDCl}_3$ .

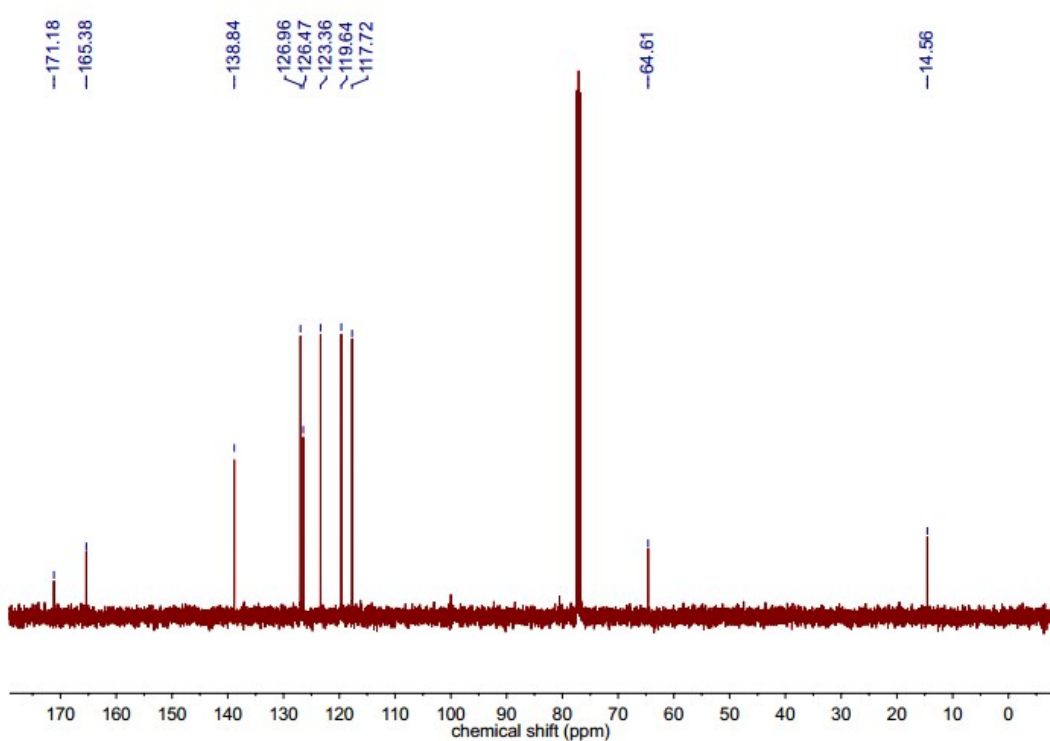


Figure S4. <sup>13</sup>C NMR spectrum of DCzOT in  $\text{CDCl}_3$ .

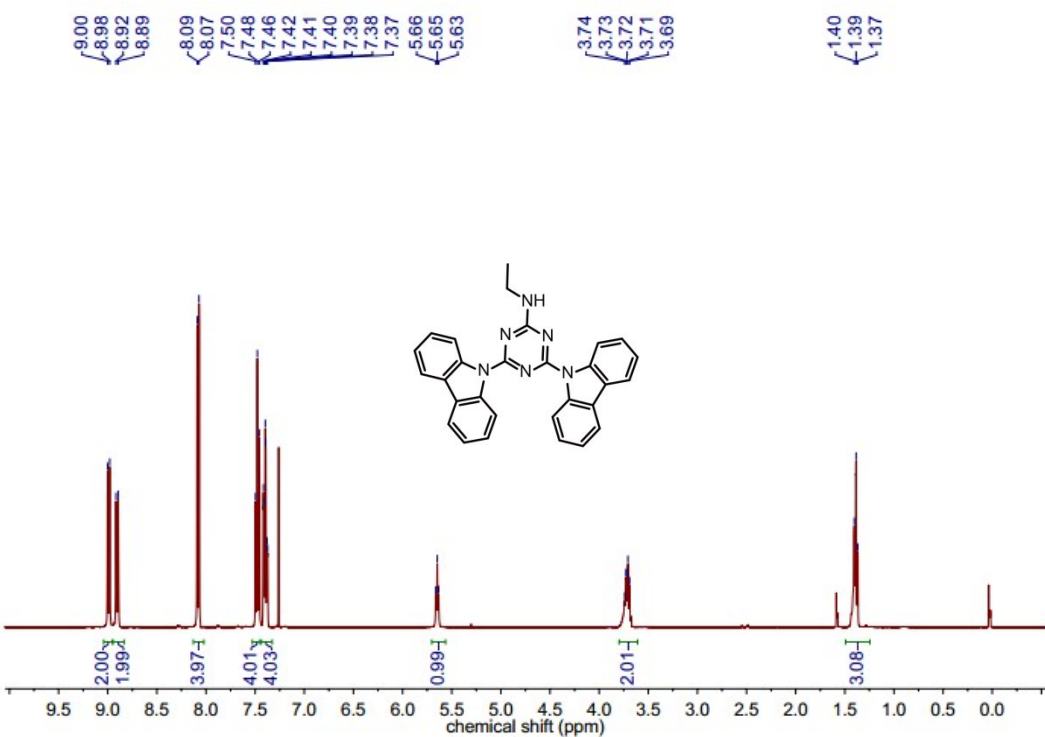
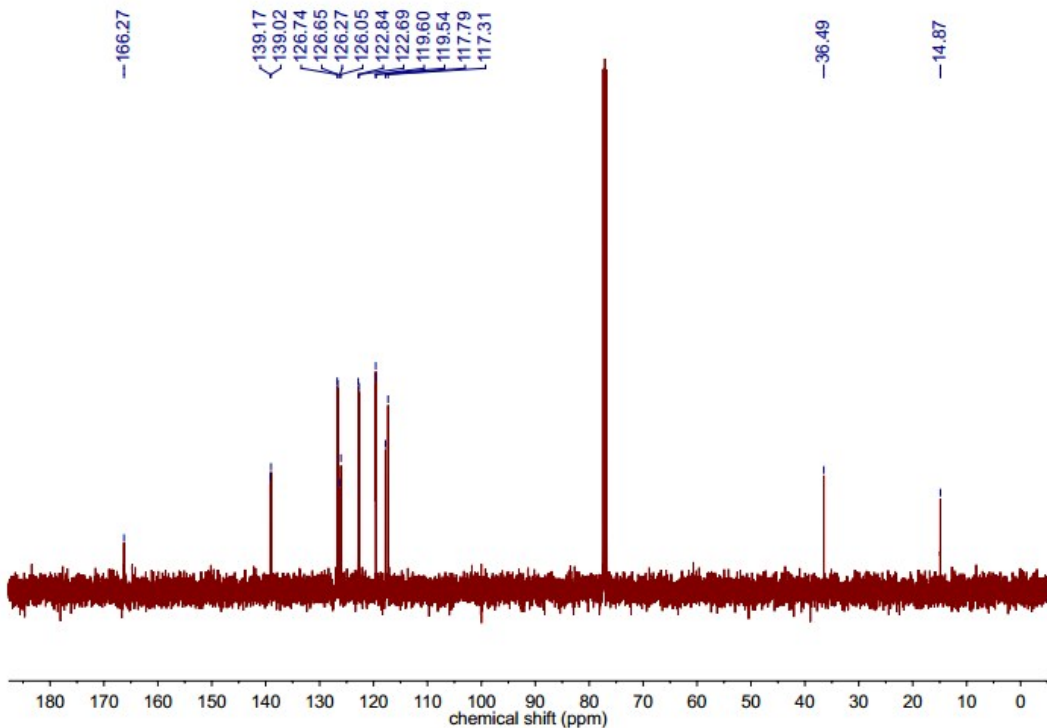
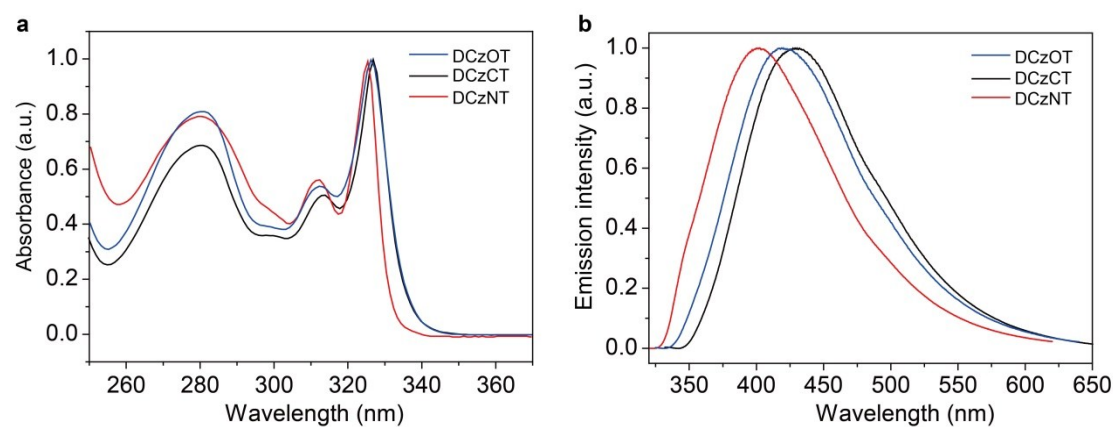


Figure S5. <sup>1</sup>H NMR spectrum of DCzNT in  $\text{CDCl}_3$ .



**Figure S6.**  $^{13}\text{C}$  NMR spectrum of DCzNT in  $\text{CDCl}_3$ .

### I. Additional photophysical properties of organic phosphors in solution and crystal state



**Figure S7.** (a) Normalized absorption and (b) the steady-state photoluminescence (PL) spectra of DCzOT, DCzCT and DCzNT in dilute chloroform solution ( $1 \times 10^{-5}$  M), respectively.

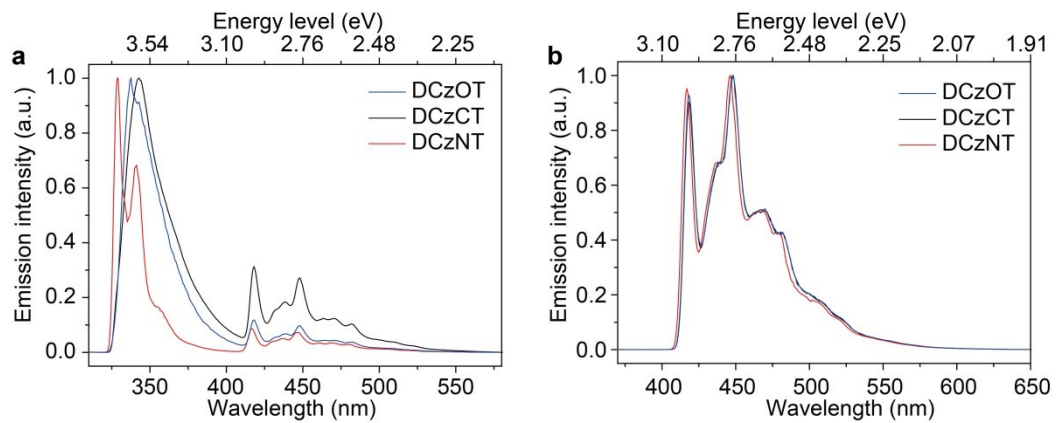


**Figure S8.** (a) The steady-state PL and (b) phosphorescence spectra of DCzOT, DCzCT and DCzNT in 2-methyltetrahydrofuran ( $1 \times 10^{-5}$  M) at 77 K, respectively.

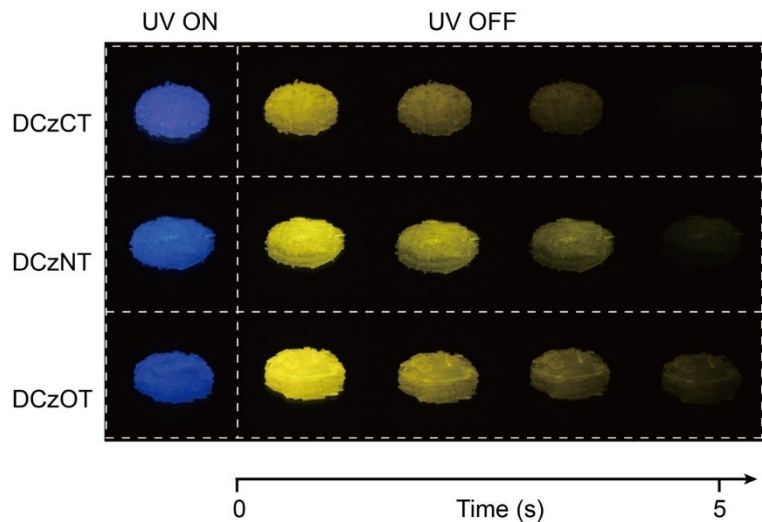


**Figure S9.** Photographs of the three ultralong organic phosphors taken at different time intervals before (first row) and after (succeeding rows) the excitation of a 365 nm UV-lamp switched off under ambient conditions.

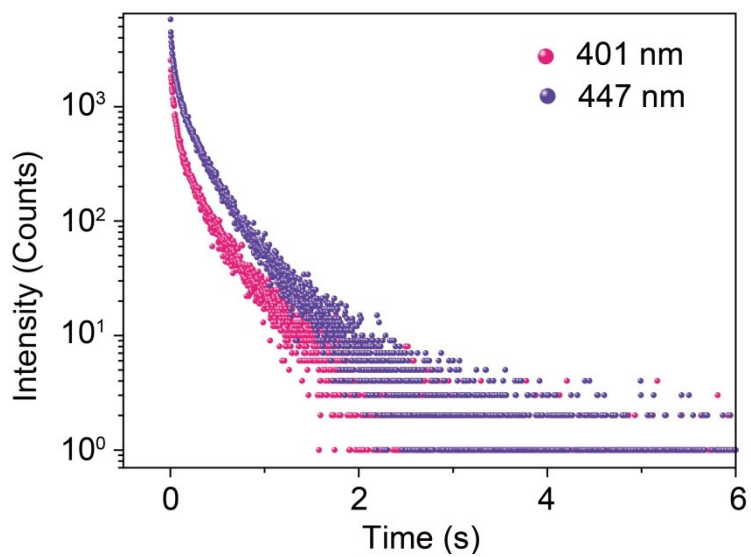


Figure S10. The lifetime decay curves of DCzOT at 401 and 447 nm in crystal under ambient conditions.

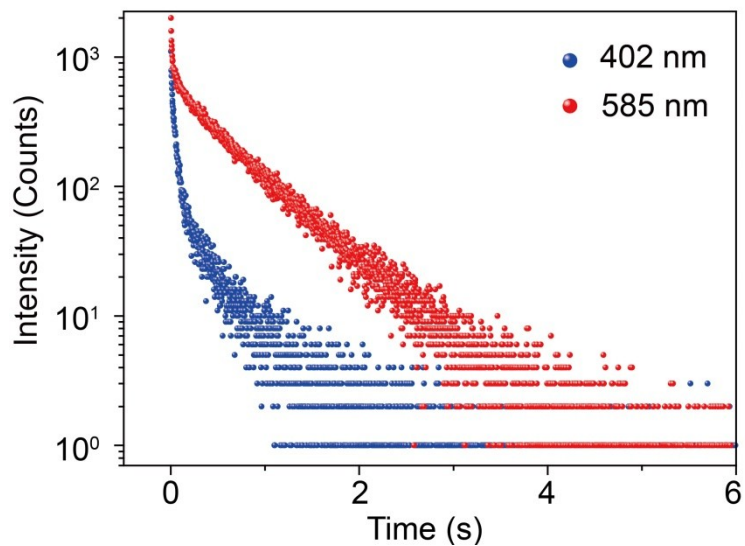
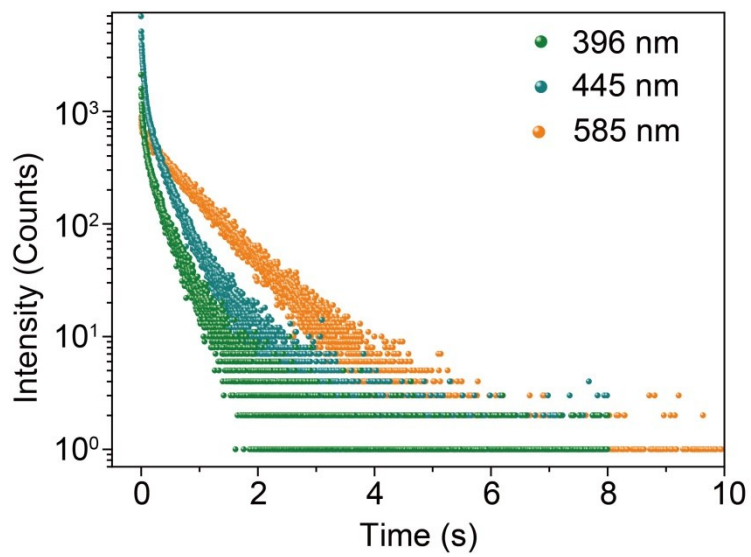
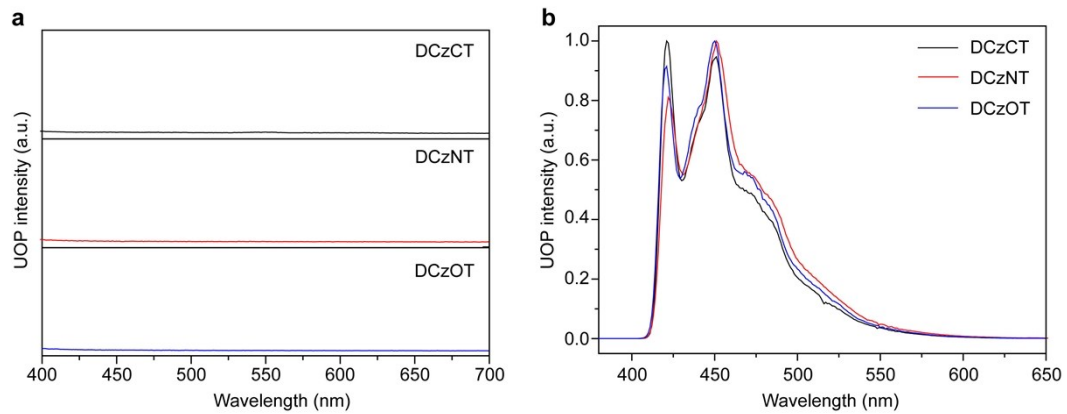


Figure S11. The lifetime decay curves of DCzCT at 402 nm and 585 nm in crystal under ambient conditions.



**Figure S12.** The lifetime decay curves of DCzNT at 396 nm, 445 nm and 585 nm in crystal at room temperature, respectively.



**Figure S13.** Phosphorescent spectra of DCzOT, DCzCT and DCzNT doped PMMA film excited by 365 nm at room temperature (a) and 77 K (b), respectively.

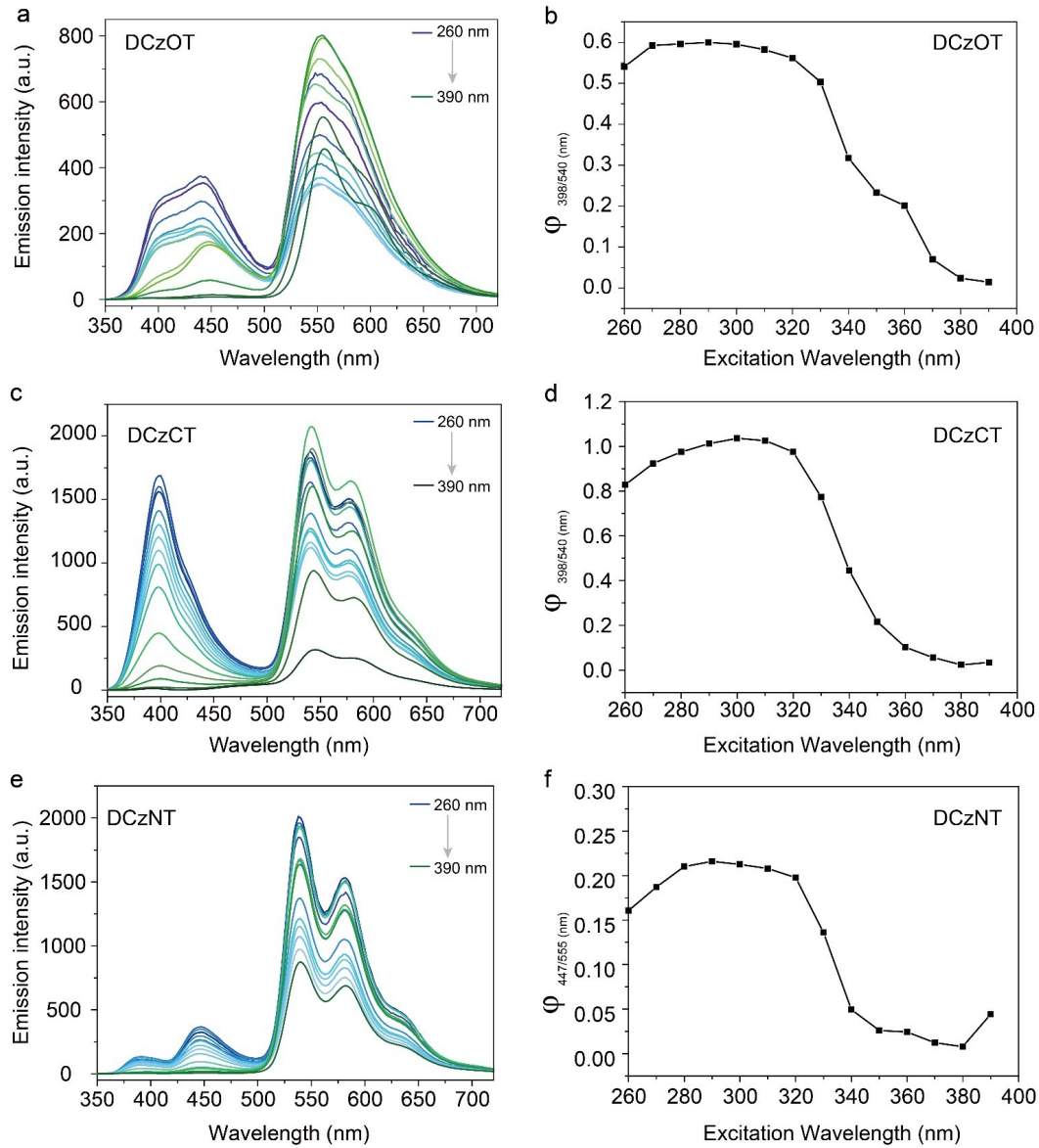


**Figure S14.** a, c and e. The phosphorescence spectra of DCzOT, DCzCT and DCzNT under different excitation ranged from 260 to 390 nm,

respectively. b, d and f. The ratio of the maximum ultralong luminescence at short wavelength bands to ultralong phosphorescence of DCzOT,

DCzCT and DCzNT, respectively.

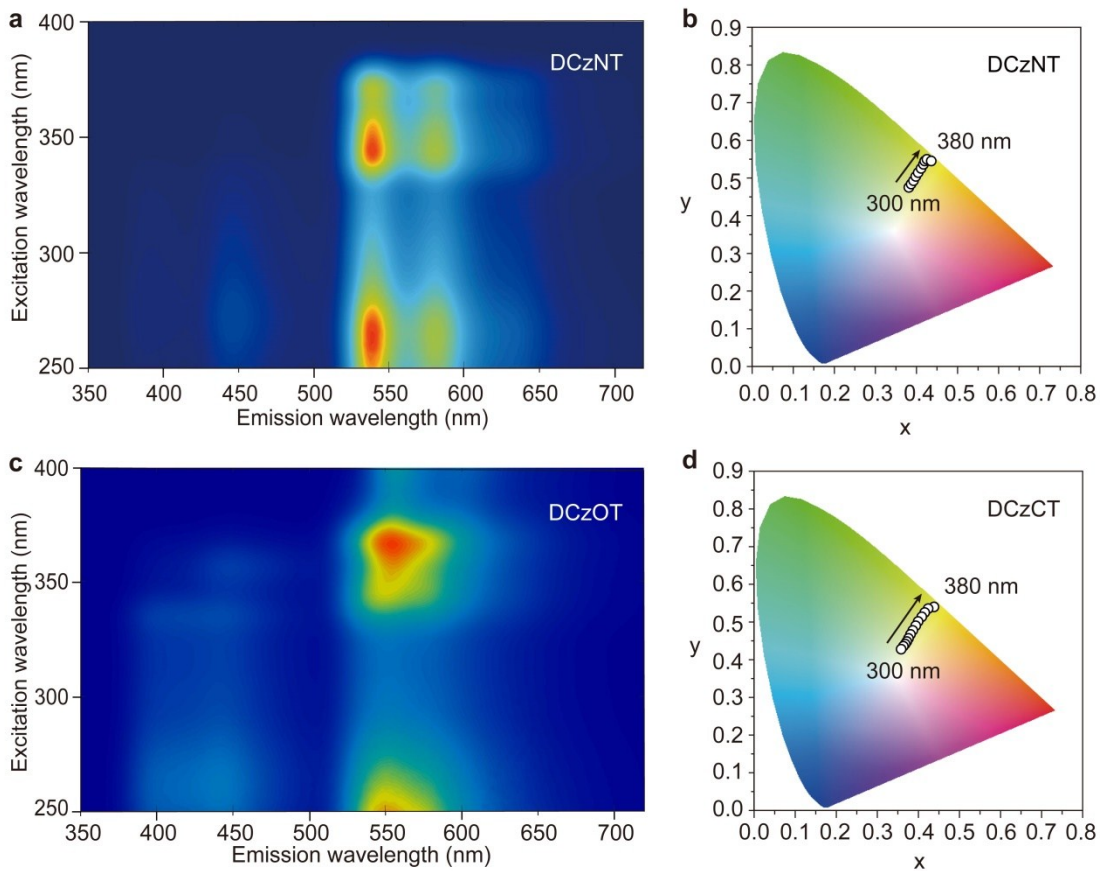


**Figure S15.** **a, c.** Solid-state excitation-phosphorescence mapping of DCzNT and DCzOT under ambient conditions. The colour change from red to green indicates the decrease in emission intensity. **b, d.** Commission Internationale de l'Eclairage (CIE) chromaticity coordinates of the ultralong luminescence for DCzNT and DCzCT powders with the excitation changed from 300 to 380 nm.

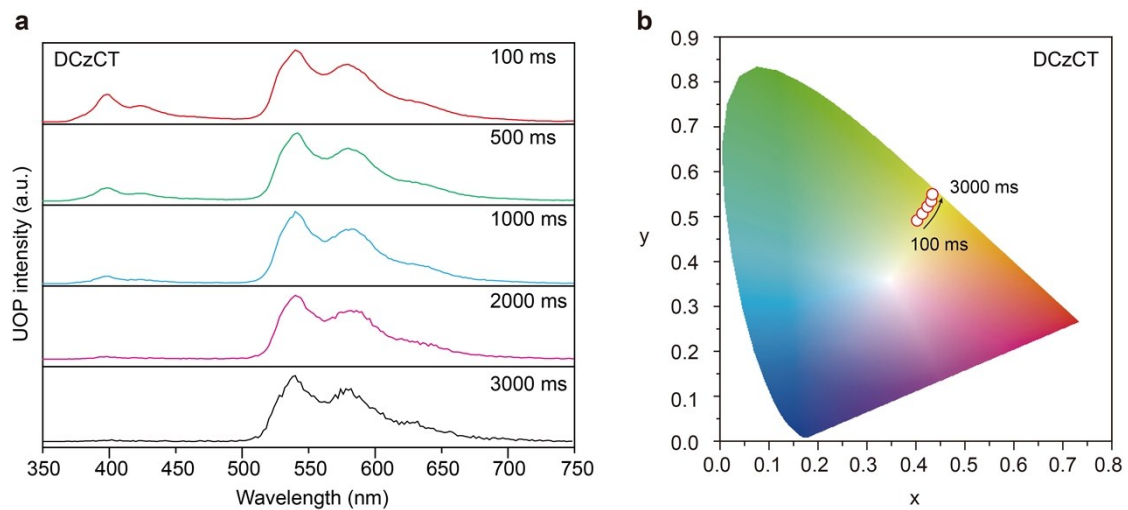


**Figure S16.** **a**, Ultralong organic phosphorescence spectra of the DCzCT powder at delay times of 100, 500, 1000, 2000, and 3000 ms, respectively. **b**, Commission Internationale de l'Eclairage (CIE) chromaticity coordinates of the ultralong luminescence for DCzCT powder at different delay time.

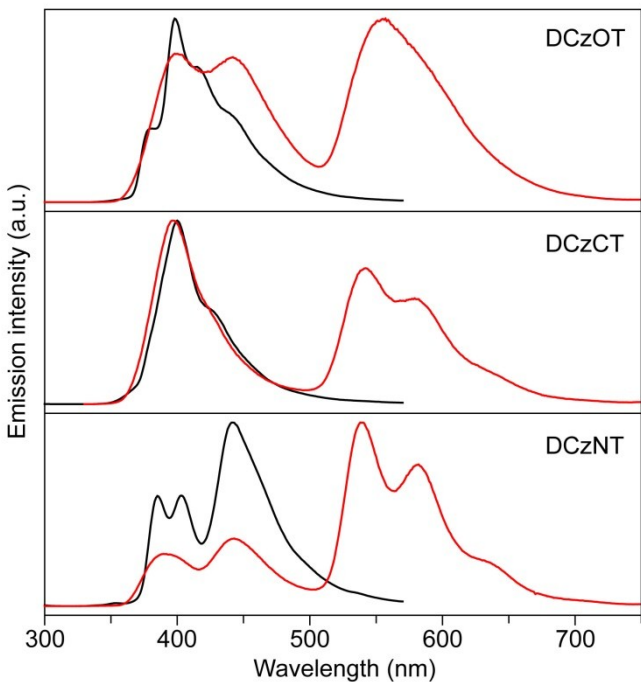


**Figure S17.** The steady-state PL (black line) and ultralong luminescence (red line) spectra of DCzOT, DCzCT and DCzNT excited by 270, 280 and 300 nm in solid states under ambient conditions, respectively.

In process of triplet–triplet annihilation (TTA), according the power law of  $I_{DF} \propto I_p^2$ , where  $I_{DF}$  and  $I_p$  are the emission intensities of delayed fluorescence and phosphorescence, respectively, the double-logarithmic relationship between the excitation power and the luminescence intensity should be observed, which deduced from the second-order kinetics of TTA. To demonstrate the emission band at around 400 nm ascribed to the delayed fluorescence emission, the dependence of the phosphorescence and delayed fluorescence intensity on excitation intensity were investigated. A similar two-fold relationship of the slop in intensity between delay fluorescence and phosphorescence in double-logarithmic plots had been found in DCzCT, which agreed with the second-order kinetics of triplet-triplet annihilation (TTA) mechanism as shown in Figure S18.

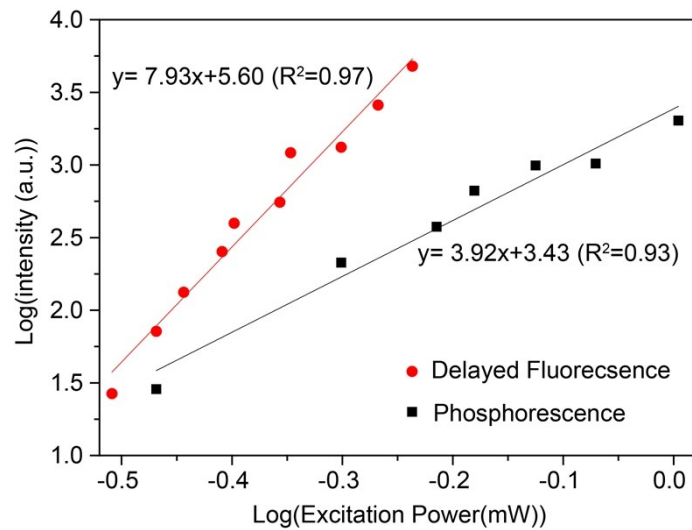


**Figure S18.** Double-logarithmic relationship between the excitation power and the luminescence intensity in DCzCT crystal. The phosphorescence intensity at 540 nm and the delayed fluorescence intensity at 398 nm excited at 350 nm were measured after shutting the excitation

### III. Theoretical calculations

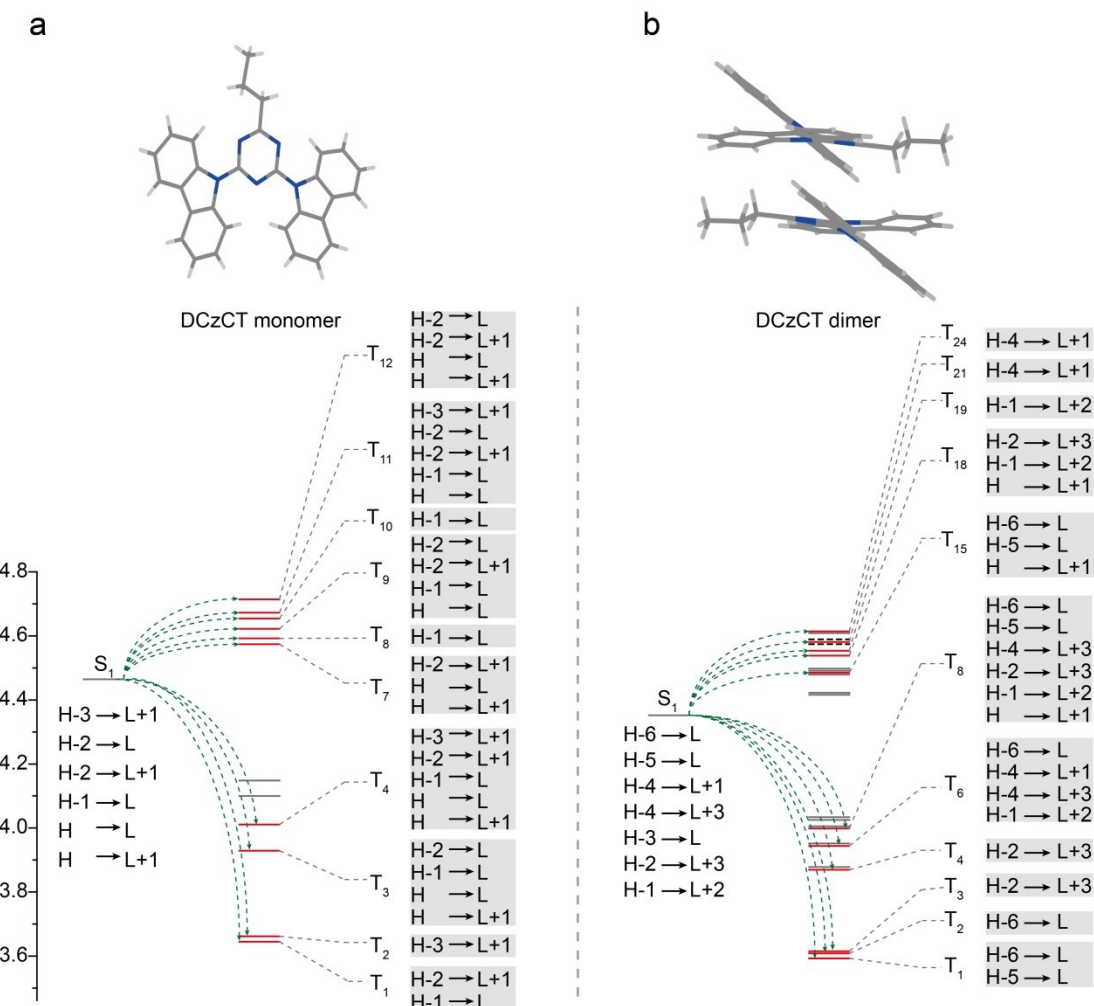


**Figure S19.** The lowest singlet ( $S_1$ ) and triplet ( $T_n$ ) states of a DCzCT monomer and its dimer obtained by TD-DFT calculations based on the single-crystal structure data of DCzCT

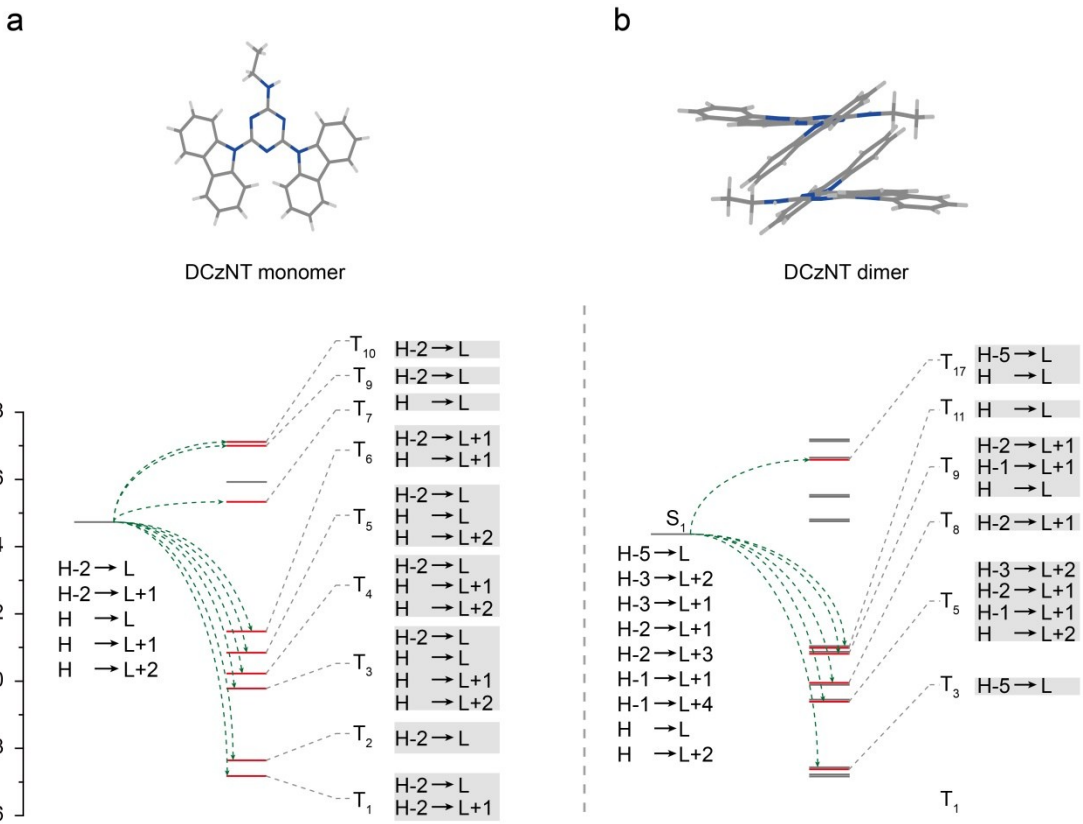


**Figure S20.** The lowest singlet ( $S_1$ ) and triplet ( $T_n$ ) states of a DCzNT monomer and its dimer obtained by TD-DFT calculations based on the single-crystal structure data of DCzNT

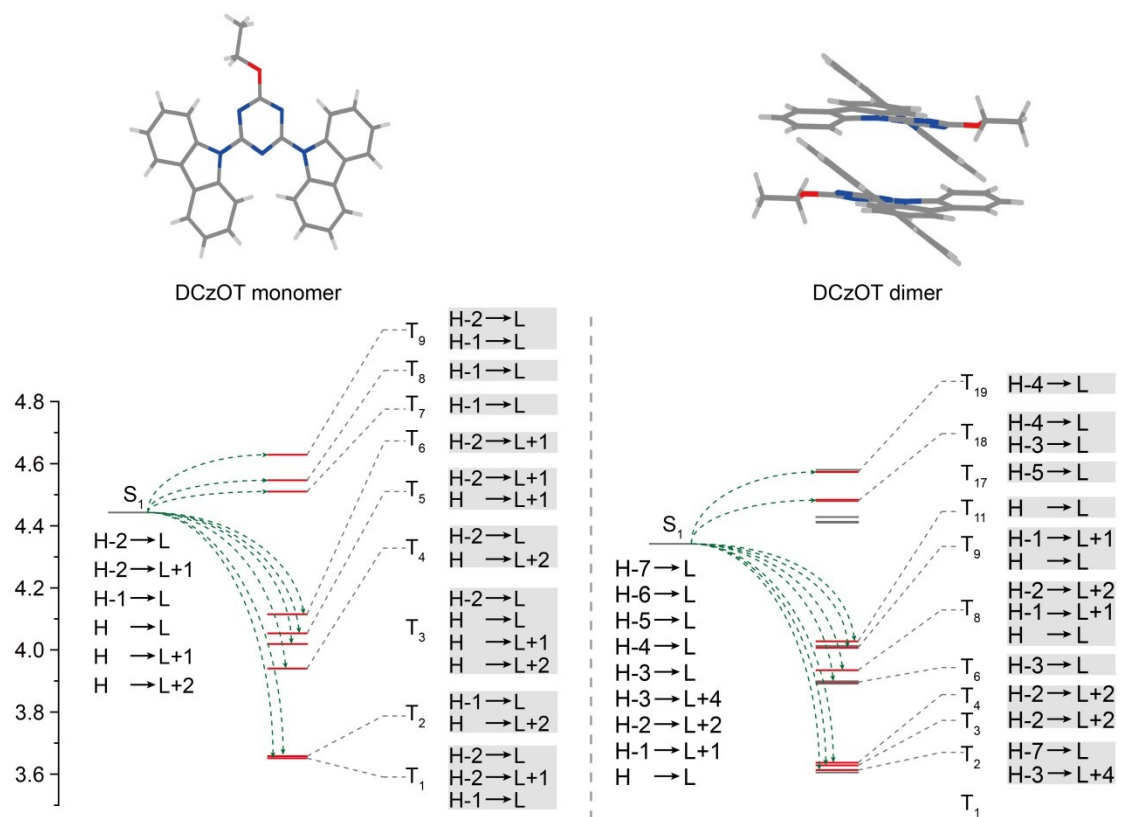


**Figure S21.** The lowest singlet ( $S_1$ ) and triplet ( $T_n$ ) states of a DCzOT monomer and its dimer obtained by TD-DFT calculations based on the single-crystal structure data of DCzOT

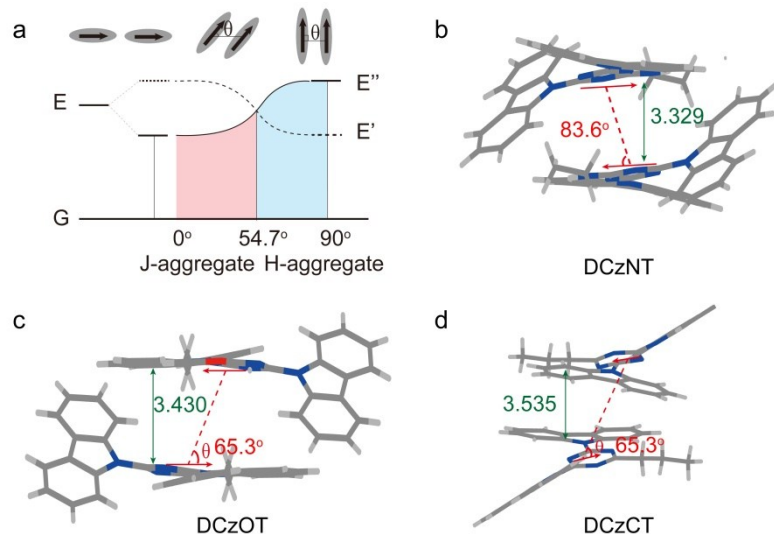


**Figure S22.** a. Schematic energy diagram of J- and H- aggregation. The H-aggregate formation of DCzNT (b), DCzOT (c) and DCzCT (d) in crystalline state. The  $\theta$  and green line represent the angle between the transition dipoles and the interconnected axis and the distance between two adjacent molecules, respectively.

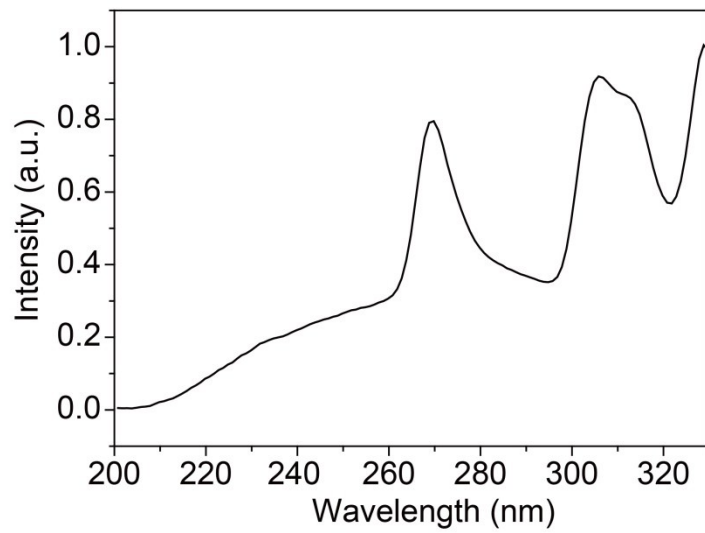


**Figure S23.** Excitation spectrum of carbazole in THF solution.

**IV. Single crystal data**

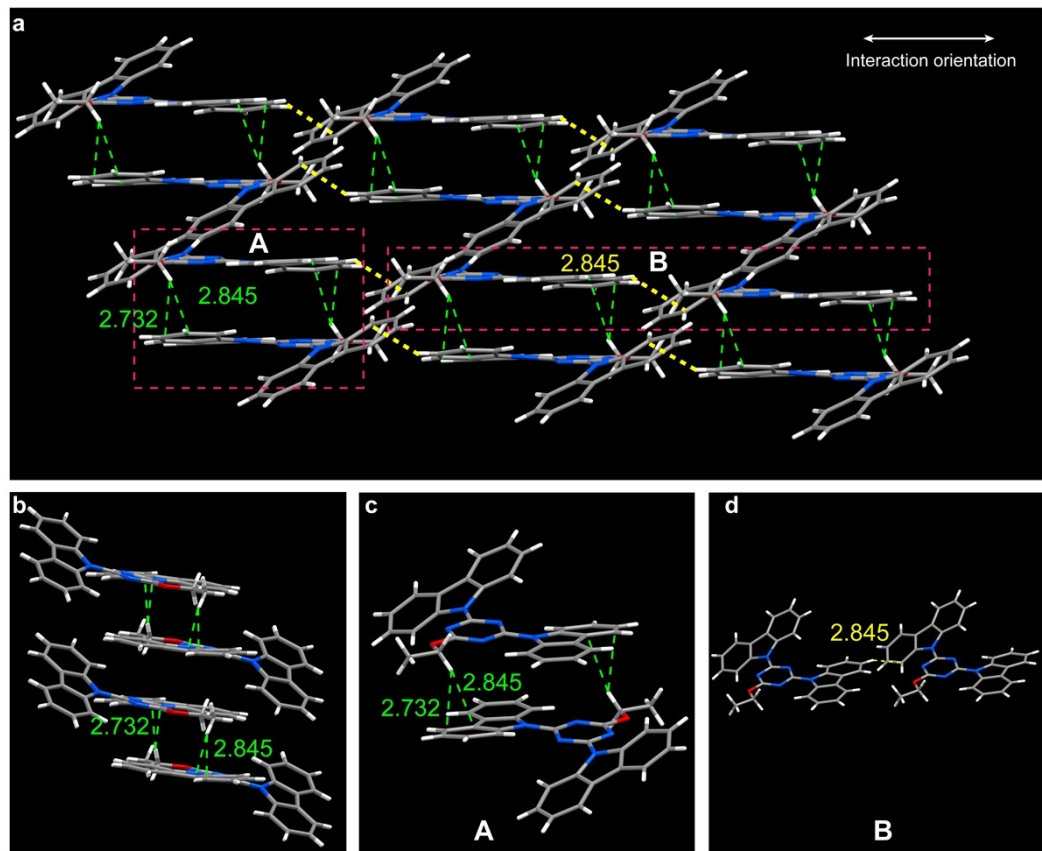


**Figure S24.** **a.** Intermolecular packing of DCzOT molecule in crystalline state. **b.** The side view of the intermolecular packing of DCzOT in crystalline state. **c** and **d** Two dimers extracted from single-crystal of DCzOT. The green dashed lines represent the distance of C-H $\cdots$  $\pi$  in each dimer. The yellow dashed lines represent the horizontal interaction between adjacent two dimers. The white arrow represents the interaction orientation in different dimes in single-crystal.

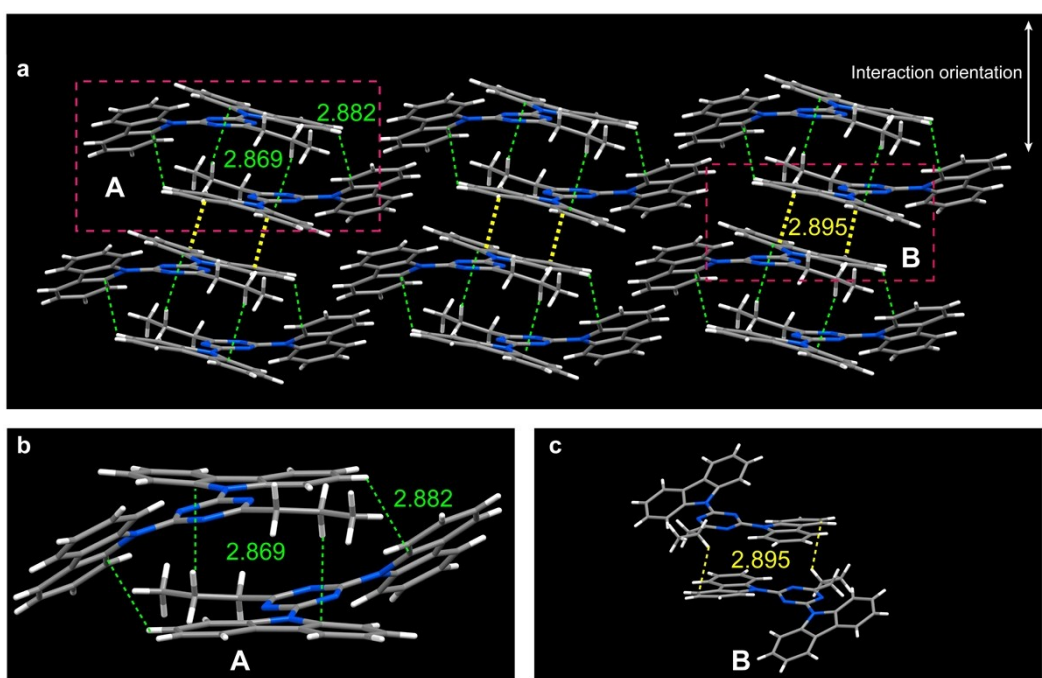


**Figure S25.** **a.** Intermolecular packing of DCzCT molecule in crystalline state. **b** and **c.** Two dimers extracted from single-crystal of DCzCT. The green dashed lines represent the distance of C-H $\cdots$  $\pi$  in each dimer. The yellow dashed lines represent the vertical interaction between adjacent two dimers. The white arrow represents the interaction orientation in different dimers in single-crystal.

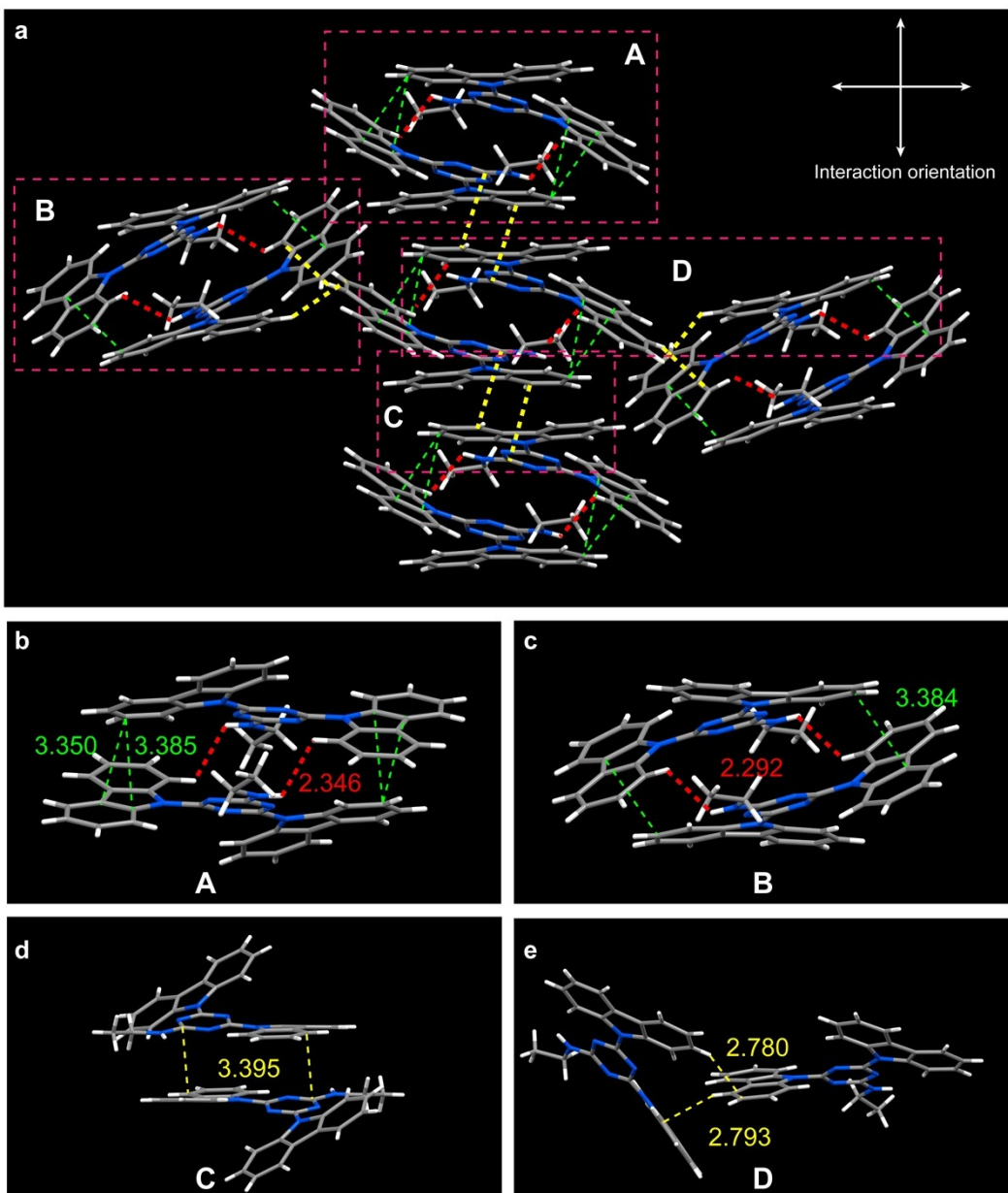


**Figure S26.** **a.** Intermolecular packing of DCzNT molecule in crystalline state. **b. c. d** and **e.** Four dimers extracted from single-crystal of DCzNT. The green dashed lines represent the distance of C-H··· $\pi$  and  $\pi$ ··· $\pi$  in each dimer. The yellow dashed lines represent the interaction between adjacent two dimers. The white arrow represents the interaction orientation in different dimeres in single-crystal.

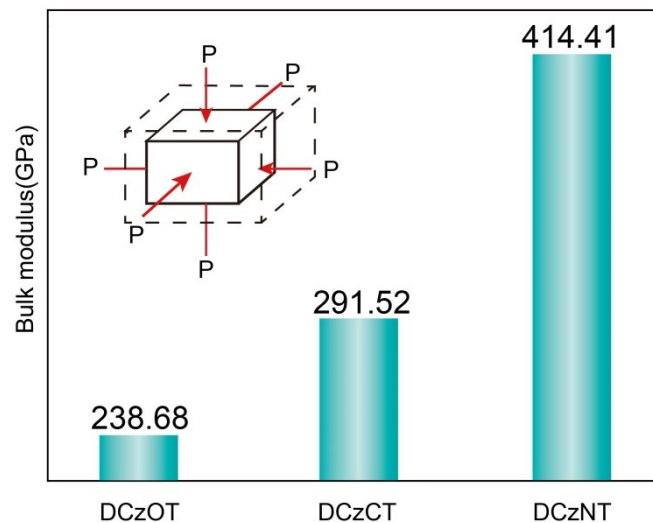


**Figure S27.** The calculated bulk modulus of DCzOT, DCzCT and DCzNT in single crystal

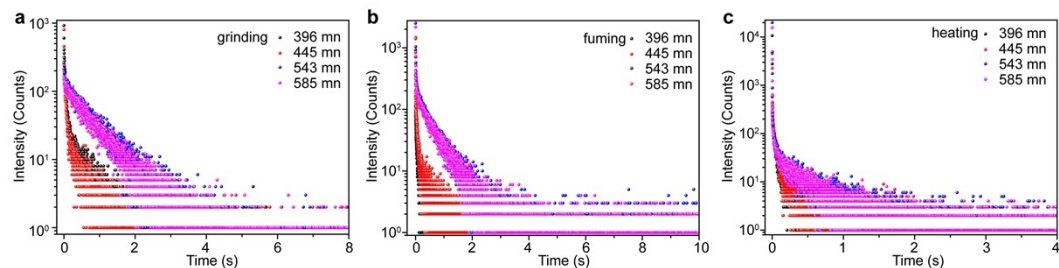


**Figure S28.** The lifetime decay curves of DCzNT crystal after grinding (a), fuming (b) and heating (c) under ambient conditions, respectively.

**Table S1.** Photophysical properties of the ultralong organic phosphors in solution crystal state.

compound	solution			crystal		
	$\lambda_{\text{abs}}$ (nm)	$\lambda_{\text{em}}$ (nm)	$\phi^{\text{a}}_{\text{fl}}$ (%)	$\lambda_{\text{em}}$ (nm)	$\phi_{\text{PL}}$ (%)	$\phi_{\text{Phos.}}$ (%)
DCzCT	280, 327	430	9.7	398	43.1	1.36
DCzNT	279, 324	401	15.4	382, 400, 439	31.3	1.7
DCzOT	279, 326	419	9.2	395, 441	45.8	1.63

a : the fluorescence quantum yield in the chloroform solution at room temperature.

**Table S2.** Photoluminescence lifetimes ( $\tau$ ) of DCzCT, DCzOT and DCzNT crystals under ambient conditions.

Compound	Wavelength (nm)	Phosphorescence					
		$\tau_1$ (ms)	A <sub>1</sub> (%)	$\tau_2$ (ms)	A <sub>2</sub> (%)	$\tau_3$ (ms)	A <sub>3</sub> (%)
DCzCT	402	37.86	44.53	341.82	55.47	-	-
	546	116.53	5.59	650.52	94.41	-	-
	585	135.20	6.00	652.49	94.00	-	-

DCzNT	396	65.00	25.40	354.24	74.60		
	445	37.38	8.79	210.26	48.23	549.27	42.98
	543	183.80	3.97	788.77	96.03	-	-
	585	189.98	3.86	792.76	96.14	-	-
DCzOT	401	34.81	18.06	160.06	43.75	453.75	43.75
	447	41.78	9.89	201.16	53.61	505.82	36.49
	553	113.62	6.68	632.60	93.32	-	-

**Table S3.** The lowest singlet state ( $S_1$ ) and triplet excited state ( $T_n$ ) transition configurations of DCzCT monomer simulated by TD-DFT calculations.

The matched excited states that contain the same orbital transition components of  $S_1$  were highlighted in red.

DCzCT	n-th	Energy (eV)	Transition configuration (%)
$S_n$	1	4.4638	H-3→L+1 (3.19), H-2→L (12.86), H-2→L+1 (12.71), H-1→L (6.57), H→L (42.43), H→L+1 (22.24),
$T_n$	1	3.6447	H-2→L+1 (4.60), H-2→L+3 (8.43), H-1→L (10.90), H-1→L+1 (24.74), H-1→L+2 (11.98), H-1→L+3 (39.35),
	2	3.6617	H-3→L (40.39), H-3→L+1 (3.95), H-3→L+2 (41.52), H-3→L+3 (6.49), H-2→L (4.26), H-2→L+2 (3.39),
	3	3.9285	H-3→L (4.53), H-2→L (49.06), H-1→L (13.60), H→L (2.83), H→L+1 (29.98)
	4	4.0104	H-3→L+1 (2.66), H-2→L (11.84), H-2→L+1 (15.64), H-1→L (5.64), H-1→L+1 (2.98), H→L (35.91), H→L+1 (25.33)
	5	4.0996	H-4→L+11 (2.84), H-3→L+3 (3.83), H-2→L+3 (7.44), H→L+2 (11.81), H→L+3 (74.09)
	6	4.1475	H-5→L+9 (3.97), H-2→L+2 (55.29), H-2→L+3 (8.37), H-1→L+2 (17.24), H-1→L+3 (2.89), H→L+2 (7.63), H→L+3 (4.61)
	7	4.5738	H-5→L+2 (2.97), H-3→L (8.68), H-3→L+2 (34.29), H-3→L+3 (8.56), H-3→L+17 (4.45), H-2→L+1 (3.24), H-2→L+2 (4.54), H-2→L+9 (10.78), H-2→L+10 (4.69), H-1→L+9 (3.14), H→L (7.06), H→L+1 (3.13), H→L+2 (4.46)
	8	4.5922	H-5→L+3 (3.90), H-4→L+3 (6.87), H-2→L+3 (2.90), H-1→L (8.51), H-1→L+1 (8.94), H-1→L+3 (36.71), H→L+8 (2.79), H→L+10 (6.87), H→L+11 (14.80), H→L+12 (7.71)
	9	4.6216	H-10→L+1 (3.64), H-5→L+2 (20.10), H-4→L+3 (10.46), H-3→L (5.07), H-2→L+1 (15.07), H-2→L+9

		(8.98), H-2→L+10 (4.60), H-1→L+1 (7.19), H→L (16.95), H→L+1 (3.07), H→L+9 (4.88)
10	4.6538	H-5→L+2 (2.98), H-5→L+3 (9.76), H-4→L+2 (8.65), H-4→L+3 (8.90), H-3→L (19.73), H-3→L+2 (4.07), H-2→L+9 (3.39), H-1→L (7.96), H-1→L+1 (17.10), H-1→L+3 (4.23), H→L+10 (3.85), H→L+11 (5.63), H→L+12 (3.74)
11	4.6725	H-10→L+1 (5.40), H-5→L+2 (4.55), H-4→L+3 (6.53), H-3→L (9.14), H-3→L+1 (10.54), H-3→L+2 (5.12), H-2→L (6.14), H-2→L+1 (23.23), H-2→L+3 (7.28), H-1→L (6.58), H→L (15.48)
12	4.7139	H-11→L+1 (5.74), H-2→L (11.19), H-2→L+1 (18.26), H-2→L+3 (5.12), H-1→L+1 (6.25), H→L (11.58), H→L+1 (37.45), H→L+2 (4.41)

**Table S4.** The lowest singlet state ( $S_1$ ) and triplet excited state ( $T_n$ ) transition configurations of DCzCT dimer simulated by TD-DFT calculations. The matched excited states that contain the same orbital transition components of  $S_1$  were highlighted in red.

DCzCT	n-th	Energy (eV)	Transition configuration (%)
$S_1$	1	4.4453	H-6→L (6.48), H-5→L (31.05), H-4→L+1 (3.01), H-4→L+3 (11.11), H-3→L (3.30), H-2→L+3 (4.76), H-1→L+2 (12.43), H→L+1 (27.86)
$T_n$	1	3.6281	H-7→L (9.43), H-7→L+1 (8.43), H-7→L+3 (8.68), H-7→L+4 (19.07), H-7→L+5 (3.75), H-6→L (28.22), H-6→L+4 (5.86), H-6→L+5 (10.97), H-5→L (5.60)
	2	3.6285	H-7→L (29.98), H-7→L+4 (5.94), H-7→L+5 (13.57), H-6→L (9.47), H-6→L+1 (8.87), H-6→L+3 (7.81), H-6→L+4 (17.04), H-6→L+5 (4.18), H-5→L+4 (3.14)
	3	3.6479	H-4→L+2 (3.04), H-4→L+6 (3.53), H-4→L+7 (2.87), H-3→L+1 (6.05), H-3→L+2 (10.49), H-3→L+3 (5.82), H-3→L+5 (3.98), H-3→L+6 (12.73), H-3→L+7 (9.06), H-2→L+1 (5.04), H-2→L+2 (9.82), H-2→L+3 (4.88), H-2→L+5 (3.72), H-2→L+6 (10.62), H-2→L+7 (8.35)
	4	3.6484	H-4→L+2 (2.91), H-4→L+6 (3.77), H-4→L+7 (2.76), H-3→L+1 (5.93), H-3→L+2 (11.41), H-3→L+3 (5.63), H-3→L+5 (4.17), H-3→L+6 (12.49), H-3→L+7 (9.91), H-2→L+1 (5.17), H-2→L+2 (9.01), H-2→L+3 (4.94), H-2→L+5 (3.29), H-2→L+6 (10.90), H-2→L+7 (7.71)
	5	3.9278	H-5→L+1 (14.45), H-5→L+3 (11.33), H-4→L (26.68), H-2→L (10.83), H-1→L+1 (16.78), H→L (8.15), H→L+2 (11.78)
	6	3.9352	H-6→L (5.05), H-5→L (29.75), H-4→L+1 (21.49), H-4→L+3 (3.57), H-2→L+1 (9.00), H-1→L (3.77), H-1→L+2 (13.44), H→L+3 (13.93)
	7	4.0075	H-5→L+1 (3.52), H-5→L+3 (4.63), H-5→L+4 (3.67), H-4→L (7.12), H-4→L+2 (4.51), H-4→L+5

		(3.92), H-3→L+1 (2.57), H-2→L (2.85), H-1→L+1 (17.63), H-1→L+3 (11.91), H-1→L+6 (2.96), H→L (13.11), H→L+2 (21.60),
8	4.0111	H-6→L (3.08), H-5→L (15.94), H-4→L+3 (11.39), H-2→L+3 (4.54), H-1→L+2 (29.43), H-1→L+5 (4.07), H→L+1 (31.55),
9	4.0673	H-6→L+4 (3.79), H-5→L+4 (24.54), H-4→L+5 (10.99), H-4→L+7 (8.87), H-2→L+5 (4.47), H-2→L+7 (3.58), H-1→L+4 (3.57), H-1→L+6 (14.48), H→L+5 (19.76), H→L+7 (5.95)
10	4.0684	H-6→L+5 (4.72), H-5→L+5 (25.65), H-5→L+7 (3.01), H-4→L+4 (24.92), H-3→L+5 (3.12), H-2→L+4 (9.81), H-1→L+7 (10.06), H→L+4 (7.75), H→L+6 (10.96)
11	4.0941	H-8→L+23 (2.96), H-5→L+5 (5.11), H-4→L+6 (8.17), H-3→L+7 (2.88), H-2→L+6 (3.51), H-1→L+5 (2.92), H-1→L+7 (35.19), H→L+1 (6.26), H→L+4 (11.55), H→L+6 (21.45)
12	4.1010	H-9→L+23 (3.45), H-5→L+4 (10.42), H-4→L+5 (10.60), H-2→L+5 (4.14), H-1→L+1 (5.43), H-1→L+6 (30.93), H→L+7 (35.04)
13	4.5151	H-11→L+4 (12.33), H-10→L+5 (11.30), H-7→L+5 (12.03), H-6→L+4 (17.07), H-5→L+4 (5.45), H-5→L+16 (9.03) H-5→L+17 (6.08), H-4→L+19 (5.64), H-4→L+21 (7.60), H→L+5 (4.35), H→L+19 (3.47), H→L+21 (5.65)
14	4.5163	H-11→L+5 (12.74), H-10→L+4 (14.36), H-7→L+4 (11.38), H-6→L+5 (12.19), H-5→L+5 (4.90), H-5→L+7 (3.46), H-5→L+19 (8.94), H-5→L+21 (11.08), H-4→L+16 (7.34), H-4→L+17 (4.94), H→L+16 (4.85), H→L+17 (3.82)
15	4.5863	H-11→L (6.03), H-11→L+5 (5.77), H-10→L+4 (7.19), H-7→L+1 (8.67), H-7→L+4 (11.38), H-7→L+31 (3.75), H-6→L (12.80), H-6→L+5 (10.67), H-5→L (7.67), H-5→L+2 (6.66), H-3→L+7 (5.82), H-2→L+6 (5.46), H→L+1 (8.13)
16	4.5889	H-11→L+4 (10.75), H-10→L (6.82), H-10→L+5 (6.92), H-7→L (10.79), H-7→L+5 (9.80), H-6→L+1 (13.90), H-6→L+4 (8.31), H-6→L+31 (4.42), H-4→L (4.39), H-4→L+2 (4.50), H-1→L+3 (4.81), H→L (14.58)
17	4.5939	H-9→L+6 (10.51), H-8→L+7 (11.62), H-4→L+7 (3.22), H-3→L+6 (14.27), H-2→L+7 (15.49), H-1→L+18 (4.01), H-1→L+23 (23.84), H→L+19 (4.45), H→L+22 (12.59)
18	4.5952	H-9→L+7 (14.68), H-8→L+6 (10.29), H-4→L+6 (4.38), H-4→L+23 (4.03), H-3→L+7 (14.25), H-2→L+6 (9.52), H-1→L+19 (5.32), H-1→L+22 (18.33), H→L+23 (19.21),
19	4.6471	H-7→L+1 (4.60), H-7→L+4 (5.00), H-6→L (5.77), H-6→L+5 (4.63), H-4→L+3 (4.58), H-3→L+2

		(3.88), H-3→L+7 (3.50), H-2→L+1 (5.07), H-2→L+3 (5.74), H-2→L+6 (4.29), H-1→L (23.28), H-1→L+2 (7.03), H-1→L+5 (8.28), H→L+1 (9.55), H→L+3 (4.80)
20	4.6626	H-9→L+6 (5.65), H-8→L+7 (4.38), H-7→L (8.52), H-7→L+5 (6.74), H-6→L+1 (3.81), H-6→L+4 (4.36), H-3→L+1 (17.73), H-3→L+6 (4.38), H-2→L+2 (16.78), H-2→L+7 (6.93), H-1→L+3 (13.18), H→L (7.54)
21	4.6828	H-9→L+7 (7.48), H-8→L+6 (7.38), H-4→L+1 (8.41), H-4→L+3 (4.16), H-4→L+6 (6.16), H-3→L+2 (18.66), H-3→L+7 (13.28), H-2→L+1 (17.29), H-2→L+31 (3.87), H-1→L (9.63), H→L+3 (3.68)
22	4.6871	H-9→L+6 (5.51), H-8→L+7 (4.29), H-4→L+2 (7.70), H-4→L+7 (4.00), H-3→L+1 (11.32), H-3→L+3 (3.81), H-3→L+6 (5.41), H-2→L (5.07), H-2→L+2 (6.23), H-2→L+7 (6.27), H-1→L+1 (8.28), H-1→L+3 (13.30), H-1→L+4 (4.01), H→L (14.79)
23	4.7208	H-6→L+1 (4.22), H-5→L+1 (24.35), H-5→L+3 (11.86), H-5→L+6 (8.41), H-4→L+2 (17.85), H-4→L+7 (6.14), H→L (7.21), H→L+2 (19.96)
24	4.7229	H-23→L+3 (2.85), H-21→L+2 (3.57), H-6→L+2 (2.98), H-5→L+2 (19.72), H-5→L+7 (5.22), H-4→L+1 (16.76), H-4→L+6 (3.32), H-2→L+1 (3.09), H-1→L (9.94), H→L+3 (25.06), H→L+6 (7.49)

**Table S5.** The lowest singlet state ( $S_1$ ) and triplet excited state ( $T_n$ ) transition configurations of DCzNT monomer simulated by TD-DFT calculations.

The matched excited states that contain the same orbital transition components of  $S_1$  were highlighted in red.

DCzNT	n-th	Energy (eV)	Transition configuration (%)
$S_n$	1	4.4736	H-2→L (9.23), H-2→L+1 (2.70), H→L (70.33), H→L+1 (12.38), H→L+2 (5.37)
$T_n$	1	3.7170	H-2→L (3.77), H-2→L+1 (5.55), H-2→L+2 (14.55), H-1→L (10.43), H-1→L+1 (14.65), H-1→L+2 (45.95), H→L+12 (5.10)
	2	3.7653	H-3→L (30.09), H-3→L+1 (54.20), H-3→L+2 (4.51), H-2→L (2.94), H-2→L+1 (5.33), H-1→L+1 (2.94)
	3	3.9772	H-2→L (18.52), H-1→L (13.41), H→L (34.55), H→L+1 (17.17), H→L+2 (10.44), H→L+4 (5.90)
	4	4.0235	H-5→L+12 (3.19), H-2→L (9.41), H-2→L+2 (4.78), H-1→L (3.64), H→L+1 (6.16), H→L+2 (61.96), H→L+4 (10.85)
	5	4.0840	H-3→L (3.62), H-2→L (34.81), H-2→L+4 (6.42), H-1→L (7.24), H→L (36.01), H→L+2 (6.25), H→L+4 (5.65)
	6	4.1479	H-6→L+10 (3.11), H-3→L+1 (9.37), H-2→L+1 (50.42), H-2→L+2 (12.26), H-1→L+1 (14.50), H-

			1→L+2 (4.37), H→L+1 (5.96)
7	4.5340		H-5→L+2 (10.83), H-5→L+4 (4.62), H-4→L+2 (3.33), H-2→L+2 (4.34), H-1→L+2 (16.53), H-1→L+4 (5.23), H→L (3.04), H→L+8 (3.58), H→L+9 (8.27), H→L+12 (40.23)
8	4.5929		H-6→L+1 (14.89), H-6→L+2 (5.58), H-4→L+1 (4.91), H-3→L+1 (16.71), H-3→L+2 (4.87), H-2→L+8 (7.03), H-2→L+9 (11.12), H-2→L+10 (19.17), H-2→L+11 (6.69), H-1→L+9 (3.29), H-1→L+10 (5.74)
9	4.6990		H-5→L+1 (4.33), H-5→L+2 (7.73), H-4→L (5.63), H-3→L (14.53), H-3→L+2 (6.08), H-3→L+4 (6.69), H-2→L (5.34), H-1→L (27.61), H-1→L+1 (3.48), H-1→L+2 (5.51), H-1→L+4 (13.09)
10	4.7099		H-6→L+1 (5.42), H-5→L+2 (6.82), H-4→L+1 (4.10), H-3→L (32.07), H-3→L+1 (6.85), H-3→L+2 (11.23), H-3→L+4 (10.74), H-2→L (8.11), H-1→L (8.49), H-1→L+4 (6.17)

**Table S6.** The lowest singlet state ( $S_1$ ) and triplet excited state ( $T_n$ ) transition configurations of DCzNT dimer simulated by TD-DFT calculations. The matched excited states that contain the same orbital transition components of  $S_1$  were highlighted in red.

DCzNT	n-th	Energy (eV)	Transition configuration (%)
$S_1$	1	4.4319	H-5→L (3.47), H-3→L+2 (3.89), H-3→L+10 (2.45), H-2→L+1 (3.88), H-2→L+3 (6.03), H-1→L+1 (31.75), H-1→L+4 (2.71), H→L (38.03), H→L+2 (7.78)
$T_n$	1	3.7124	H-7→L+1 (7.38), H-7→L+3 (15.86), H-6→L+2 (22.14), H-5→L+1 (13.06), H-5→L+3 (13.36), H-4→L+2 (25.18), H-1→L+19 (3.03)
	2	3.7130	H-7→L+2 (21.03), H-6→L+1 (10.04), H-6→L+3 (15.60), H-5→L+2 (24.08), H-4→L+1 (11.47), H-4→L+3 (15.00), H-1→L+17 (2.79)
	3	3.7379	H-7→L (5.84), H-7→L+5 (16.31), H-6→L+1 (9.10), H-6→L+3 (4.15), H-6→L+4 (8.88), H-5→L (4.73), H-5→L+5 (11.73), H-4→L+1 (9.00), H-4→L+3 (5.50), H-4→L+4 (9.52), H-3→L+5 (4.47), H-2→L+1 (3.07), H-2→L+4 (3.57), H→L+5 (4.14)
	4	3.7381	H-7→L+1 (13.61), H-7→L+3 (3.23), H-7→L+4 (10.81), H-6→L (5.03), H-6→L+5 (15.76), H-5→L+1 (4.81), H-5→L+3 (6.68), H-5→L+4 (7.56), H-4→L (8.09), H-4→L+5 (17.96), H-2→L+5 (6.46)
	5	3.9397	H-3→L (3.90), H-3→L+2 (9.28), H-2→L+1 (4.87), H-1→L+1 (17.14), H-1→L+3 (27.37), H→L+2 (37.43)
	6	3.9405	H-3→L+1 (8.89), H-3→L+3 (4.51), H-2→L+2 (2.59), H-1→L+2 (43.73), H→L+1 (14.93), H→L+3 (25.35)
	7	3.9838	H-4→L (3.18), H-3→L+1 (23.34), H-3→L+3 (9.32), H-3→L+4 (6.87), H-2→L (40.58), H-1→L (4.44),

		H-1→L+10 (5.45), H→L+4 (3.62), H→L+8 (3.20)
8	3.9899	H-3→L (44.58), H-2→L+1 (24.46), H-2→L+3 (9.72), H-2→L+4 (4.80), H-1→L+4 (6.07), H-1→L+8 (3.49), H→L+10 (6.89)
9	4.0759	H-5→L (5.05), H-3→L+5 (4.72), H-3→L+10 (5.15), H-2→L+1 (10.42), H-2→L+3 (6.06), H-2→L+4 (3.78), H-1→L+1 (17.47), H-1→L+4 (5.27), H→L (42.08)
10	4.0820	H-5→L+1 (5.87), H-3→L+1 (4.50), H-3→L+3 (4.59), H-3→L+4 (8.73), H-2→L (6.81), H-2→L+5 (10.21), H-2→L+10 (3.64), H-1→L (32.23), H→L+1 (19.70), H→L+3 (3.72)
11	4.0969	H-10→L+21 (3.73), H-5→L+5 (8.72), H-3→L+5 (27.21), H-2→L+4 (28.56), H-2→L+8 (5.07), H-1→L+4 (9.94), H→L (4.66), H→L+5 (12.11)
12	4.0992	H-10→L+22 (3.60), H-5→L+4 (6.81), H-3→L+4 (16.68), H-3→L+8 (5.05), H-2→L+5 (33.88), H-1→L (8.28), H-1→L+5 (7.42), H→L+4 (18.29)
13	4.4757	H-12→L+2 (10.89), H-11→L+3 (6.52), H-11→L+4 (3.69), H-6→L+2 (5.34), H-5→L+3 (5.34), H-4→L+2 (6.95), H-3→L+17 (7.15), H-1→L+19 (27.17), H→L+17 (21.96), H→L+21 (4.99)
14	4.4761	H-12→L+3 (8.05), H-12→L+4 (4.23), H-11→L+2 (8.89), H-7→L+2 (5.13), H-5→L+2 (6.26), H-4→L+3 (5.58), H-3→L+19 (6.86), H-1→L+17 (26.51), H-1→L+21 (5.16), H→L+19 (23.33)
15	4.5484	H-13→L+4 (6.23), H-10→L+5 (17.31), H-9→L+4 (6.64), H-7→L+4 (4.40), H-6→L+5 (5.74), H-5→L+4 (3.95), H-4→L+5 (6.83), H-3→L+17 (4.68), H-3→L+21 (12.64), H-2→L+16 (3.62), H-2→L+20 (7.78), H-2→L+22 (16.19), H→L+21 (3.98)
16	4.5486	H-13→L+5 (7.60), H-10→L+4 (14.84), H-9→L+5 (8.22), H-7→L+5 (6.51), H-6→L+4 (4.32), H-5→L+5 (5.11), H-4→L+4 (5.84), H-3→L+20 (6.01), H-3→L+22 (11.65), H-2→L+17 (7.68), H-2→L+21 (17.79), H→L+22 (4.43)
17	4.6533	H-10→L+1 (3.34), H-10→L+4 (3.68), H-9→L (5.63), H-7→L (8.15), H-7→L+5 (5.01), H-7→L+10 (6.39), H-6→L+1 (8.81), H-6→L+4 (9.63), H-5→L (15.12), H-5→L+5 (6.44), H-5→L+10 (3.81), H-4→L+1 (6.82), H-4→L+4 (4.60), H-4→L+8 (4.72), H-3→L (3.89), H→L (3.97)
18	4.6567	H-10→L+5 (6.91), H-9→L+1 (4.58), H-7→L+1 (8.62), H-7→L+4 (7.54), H-6→L (15.01), H-6→L+5 (7.03), H-6→L+10 (5.22), H-5→L+1 (7.74), H-5→L+4 (8.45), H-4→L (14.94), H-4→L+5 (6.70), H-4→L+10 (7.25)
19	4.7080	H-12→L+2 (10.88), H-11→L+1 (4.74), H-11→L+3 (6.27), H-8→L (19.82), H-8→L+10 (12.12), H-7→L+4 (7.36), H-6→L (11.44), H-5→L+4 (4.62), H-4→L (22.74)

	20	4.7140	H-12→L+1 (4.94), H-12→L+3 (6.72), H-11→L+2 (9.37), H-9→L (4.93), H-9→L+10 (4.42), H-8→L+8 (4.16), H-7→L (20.10), H-6→L+8 (3.78), H-5→L (8.34), H-5→L+10 (3.91), H-4→L+1 (9.04), H-4→L+4 (12.36), H-3→L (3.82), H-3→L+10 (4.12)
--	----	--------	--

**Table S7.** The lowest singlet state ( $S_1$ ) and triplet excited state ( $T_n$ ) transition configurations of DCzOT monomer simulated by TD-DFT calculations.

The matched excited states that contain the same orbital transition components of  $S_1$  were highlighted in red.

DCzOT	n-th	Energy (eV)	Transition configuration (%)
$S_n$	1	4.4413	H-2→L (14.83), H-2→L+1 (4.73), H-1→L (6.46), H→L (58.32), H→L+1 (11.12), H→L+2 (4.54)
$T_n$	1	3.6528	H-3→L (27.31), H-3→L+1 (38.54), H-2→L (7.45), H-2→L+1 (14.20), H-2→L+7 (3.90), H-1→L (3.65), H-1→L+2 (4.95),
	2	3.6562	H-2→L+2 (6.56), H-1→L (7.45), H-1→L+1 (16.67), H-1→L+2 (61.17), H-1→L+3 (4.00), H→L+2 (4.15)
	3	3.9401	H-11→L (2.51), H-3→L (5.99), H-2→L (50.03), H→L (18.04), H→L+1 (12.09), H→L+2 (3.07), H→L+3 (8.28)
	4	4.0191	H-4→L+10 (3.33), H-4→L+11 (3.62), H-2→L (3.87), H-2→L+3 (4.09), H→L (12.84), H→L+2 (48.42), H→L+3 (23.84)
	5	4.0534	H-5→L+7 (8.09), H-3→L (4.22), H-3→L+1 (17.73), H-2→L+1 (45.17), H-2→L+2 (9.47), H-2→L+3 (4.10), H-1→L+1 (6.37), H→L+1 (4.85)
	6	4.1138	H-5→L+1 (12.70), H-5→L+2 (5.40), H-5→L+3 (4.27), H-5→L+18 (2.51), H-3→L+1 (15.04), H-3→L+2 (5.39), H-3→L+3 (2.79), H-3→L+7 (4.67), H-2→L+1 (3.29), H-2→L+7 (33.55), H-2→L+9 (2.96), H-1→L+7 (4.43), H→L+7 (3.00)
	7	4.5457	H-4→L+2 (12.59), H-4→L+3 (10.64), H-1→L (3.03), H-1→L+2 (13.72), H-1→L+3 (10.27), H→L+10 (20.15), H→L+11 (20.32), H→L+12 (9.28)
	8	4.5494	H-7→L+7 (3.77), H-5→L (3.40), H-5→L+1 (11.62), H-4→L+2 (3.40), H-3→L (28.28), H-3→L+1 (6.03), H-3→L+2 (9.99), H-3→L+3 (8.90), H-3→L+18 (3.70), H-2→L+7 (3.01), H-1→L (11.92), H-1→L+1 (2.78), H-1→L+3 (3.20)

	9	4.6283	H-4→L+2 (14.50), H-3→L (10.21), H-2→L (7.89), H-1→L (32.41), H-1→L+1 (9.88), H-1→L+3 (20.77), H-1→L+18 (4.33)
--	---	--------	--

**Table S8.** The lowest singlet state ( $S_1$ ) and triplet excited state ( $T_n$ ) transition configurations of DCzOT dimer simulated by TD-DFT calculations. The matched excited states that contain the same orbital transition components of  $S_1$  were highlighted in red.

DCzCT	n-th	Energy(eV)	Transition configuration (%)
$S_1$	1	4.4181	H-7→L (3.22), H-4→L (2.77), H-3→L (3.87), H-3→L+4 (4.24), H-2→L+2 (7.54), H-1→L+1 (35.6), H→L (42.76)
$T_n$	1	3.6241	H-7→L+1 (12.24), H-7→L+2 (5.56), H-7→L+4 (4.02), H-7→L+5 (6.32), H-6→L+4 (6.27), H-5→L (5.68), H-5→L+1 (3.87), H-5→L+4 (24.02), H-4→L+1 (5.56), H-3→L+1 (6.51), H-3→L+5 (4.65), H- 2→L+4 (6.51), H-1→L+4 (4.34), H→L+1 (4.46)
	2	3.6245	H-7→L (8.89), H-7→L+4 (9.19), H-6→L+1 (8.96), H-5→L+1 (8.96), H-5→L+2 (9.04), H-5→L+4 (9.19), H-5→L+5 (9.26), H-4→L+4 (9.19), H-3→L+4 (9.19), H-2→L+1 (8.96), H→L+4(9.19)
	3	3.6552	H-7→L+2 (9.05), H-7→L+3 (9.13), H-6→L+2 (9.05), H-6→L+3 (9.13), H-6→L+4 (9.2), H-5→L+2 (9.05), H-5→L+3 (9.13), H-4→L+2 (9.05), H-4→L+3 (9.13), H-3→L+2 (9.05), H-2→L+2 (9.05)
	4	3.6561	H-7→L+2 (11.07), H-7→L+3 (11.16), H-6→L+2 (11.07), H-6→L+3 (11.16), H-5→L+2 (11.07), H- 5→L+3 (11.16), H-4→L+2 (11.07), H-4→L+3 (11.16), H-2→L+2 (11.07)
	5	3.9294	H-6→L(9.79), H-4→L+1 (9.88), H-3→L+1 (9.88), H-3→L+5 (10.21), H-2→L(9.79), H-1→L(9.79), H- 1→L+3 (10.04), H-1→L+7 (10.38), H→L+2 (9.96), H→L+6 (10.29)
	6	3.9368	H-6→L+1 (9.84), H-4→L(9.76), H-3→L(9.76), H-2→L+1 (9.84), H-2→L+5 (10.17), H-1→L+2 (9.92), H-1→L+6 (10.26), H→L+3 (10.01), H→L+4 (10.09), H→L+7 (10.34)
	7	3.9778	H-3→L+2 (11.05), H-2→L+3 (11.14), H-2→L+4 (11.23), H-1→L(10.87), H-1→L+3 (11.14), H-1→L+4 (11.23), H→L+1 (10.96), H→L+2 (11.05), H→L+5 (11.33)
	8	3.9791	H-3→L+3 (11.13), H-2→L+2 (11.04), H-2→L+5 (11.32), H-1→L+1 (10.95), H-1→L+2 (11.04), H- 1→L+5 (11.32), H→L(10.86), H→L+3 (11.13), H→L+4 (11.22)
	9	4.0569	H-7→L(9.68), H-4→L+4 (10.01), H-3→L+4 (10.01), H-3→L+7 (10.26), H-2→L+5 (10.09), H-2→L+6 (10.17), H-1→L+1 (9.76), H-1→L+5 (10.09), H→L(9.68), H→L+7 (10.26)
	10	4.0616	H-3→L+5 (14.47), H-3→L+6 (14.59), H-2→L(13.88), H-2→L+7 (14.71), H-1→L(13.88), H→L+1 (14), H→L+5 (14.47)

	11	4.0783	H-7→L+4 (7.7), H-6→L+5 (7.77), H-4→L+4 (7.7), H-3→L+3 (7.64), H-3→L+4 (7.7), H-2→L+1 (7.51), H-2→L+5 (7.77), H-2→L+6 (7.83), H-1→L+5 (7.77), H-1→L+6 (7.83), H→L(7.45), H→L+3 (7.64), H→L+4 (7.7)
	12	4.0786	H-6→L+4 (8.35), H-5→L+4 (8.35), H-4→L+1 (8.15), H-4→L+5 (8.42), H-3→L+1 (8.15), H-3→L+5 (8.42), H-3→L+6 (8.49), H-2→L+3 (8.28), H-2→L+4 (8.35), H-1→L+3 (8.28), H-1→L+4 (8.35), H→L+5 (8.42)
	13	4.4914	H-9→L+3 (6.68), H-9→L+4 (6.74), H-8→L+5 (6.8), H-8→L+6 (6.85), H-7→L+4 (6.74), H-6→L+5 (6.8), H-5→L+5 (6.8), H-3→L+15 (7.36), H-3→L+21 (7.72), H-2→L+16 (7.42), H-2→L+20 (7.66), H-1→L+16 (7.42), H-1→L+20 (7.66), H→L+15 (7.36)
	14	4.4932	H-9→L+5 (6.36), H-9→L+6 (6.41), H-8→L+3 (6.25), H-8→L+4 (6.3), H-7→L+5 (6.36), H-7→L+6 (6.41), H-5→L+4 (6.3), H-4→L+5 (6.36), H-3→L+16 (6.94), H-3→L+20 (7.16), H-2→L+15 (6.89), H-2→L+21 (7.22), H-1→L+15 (6.89), H-1→L+21 (7.22), H→L+16 (6.94)
	15	4.5109	H-11→L+3→ (8.43), H-11→L+5 (8.57), H-10→L+3 (8.43), H-4→L+3 (8.43), H-2→L+15 (9.29), H-2→L+18 (9.51), H-1→L+15 (9.29), H-1→L+18 (9.51), H→L+15 (9.29), H→L+18 (9.51), H→L+21 (9.73)
	16	4.5111	H-11→L+3 (7.08), H-10→L+2 (7.02), H-10→L+3 (7.08), H-10→L+5 (7.19), H-3→L+18 (7.98), H-2→L+15 (7.79), H-2→L+18 (7.98), H-1→L+15 (7.79), H-1→L+18 (7.98), H-1→L+21 (8.17), H→L+15 (7.79), H→L+18 (7.98), H→L+21→(8.17)
	17	4.5665	H-9→L+1 (10.92), H-8→L+4 (11.19), H-7→L+1 (10.92), H-7→L+6(11.38), H-6→L(10.83), H-5→L(10.83), H-5→L+3 (11.1), H-5→L+7 (11.47), H-4→L+6 (11.38)
	18	4.5668	H-9→L+4 (9.19), H-8→L+1 (8.97), H-7→L(8.89),H-7→L+3 (9.12), H-7→L+7 (9.42), H-6→L+1 (8.97), H-6→L+6 (9.34), H-5→L+1 (8.97), H-5→L+6 (9.34), H-4→L(8.89), H-3→L(8.89)
	19	4.6672	H-11→L+2 (8.25), H-10→L+3 (8.32), H-8→L+2 (8.25), H-7→L(8.11), H-7→L+7 (8.59), H-6→L+1 (8.18), H-6→L+5 (8.45), H-6→L+6 (8.52), H-5→L+1 (8.18), H-5→L+5 (8.45), H-4→L (8.11), H-4→L+7 (8.59)
	20	4.6676	H-11→L+3 (9.1), H-10→L+2 (9.03), H-7→L+1 (8.95), H-7→L+5 (9.25), H-6→L(8.88), H-6→L+7 (9.41), H-5→L(8.88), H-5→L+7 (9.41), H-4→L+1 (8.95), H-4→L+5 (9.25), H-2→L (8.88)

**Table S9.** The types and number of the leading intermolecular interactions in minimum units for DCzOT, DCzCT and DCzNT in crystal states.

Compounds	Horizontal orientation			Vertical orientation			
	types	distance	number	types	distance	number	
DCzOT	C-H···π	2.723 Å	2	-	-	-	
		2.846 Å	2	-	-	-	
		2.854 Å	2	-	-	-	
DCzCT	-	-	-	C-H···π	2.869 Å	2	
	-	-	-		2.895 Å	2	
	-	-	-		2.882 Å	2	
DCzNT	C-H···H-N		2.292 Å	2	π···π	3.395 Å	2
			2.346 Å	2	-	-	-
	C-H···π		2.780 Å	2	-	-	-
			3.384 Å	2	-	-	-
	π···π		3.350 Å	2	-	-	-
			3.385 Å	2	-	-	-

**Table S10.** Structure data of DCzOT, DCzCT and DCzNT single crystals

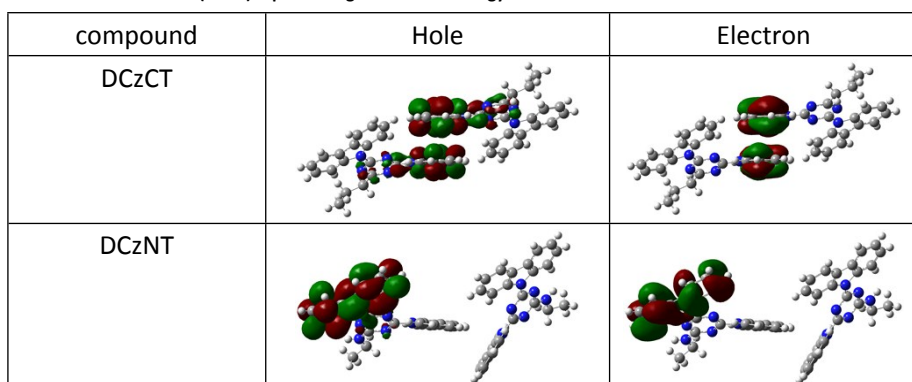
Name	DCzOT	DCzCT	DCzNT
Formula	C <sub>29</sub> H <sub>21</sub> N <sub>5</sub> O	C <sub>30</sub> H <sub>23</sub> N <sub>5</sub>	C <sub>29</sub> H <sub>22</sub> N <sub>6</sub>
Wavelength (Å)	0.71073	0.71073	0.71073
Space Group	P-1	P-1	P-1
Cell Lengths (Å)	a=7.661(3) b=10.946(5) c=14.260(6)	a=7.6238(15) b=11.162(2) c=14.418(3)	a=7.9989(16) b=11.385(2) c=25.451(5)
Cell Angles (°)	α 72.721(5) β 84.178(6) γ 77.936(5)	α 70.743(3) β 82.690(3) γ 78.468(3)	α 84.99(3) β 89.04(3) γ 77.47(3)
Cell Volume (Å <sup>3</sup> )	1115.6(8)	1132.4(4)	2254.0(8)

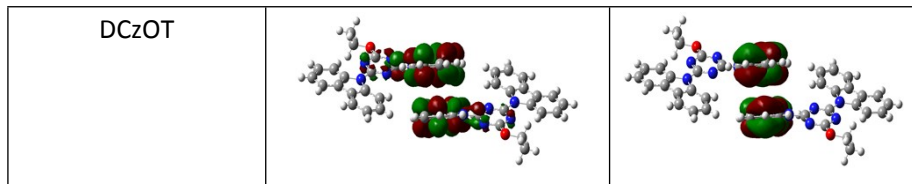
$Z$	2	2	4
Density (g/cm <sup>3</sup> )	1.356	1.330	1.339
F(000)	476.0	476.0	952.0
$h_{\max}$ , $k_{\max}$ , $l_{\max}$	9,13,16	9,13,17	9,13,30
$T_{\min}$ , $T_{\max}$	0.990, 0.992	0.924, 0.953	0.734, 0.796
CCDC	1542236	1542224	1542150

**Table S11.** Photoluminescence lifetimes ( $\tau$ ) of DCzNT crystals after grinding, fuming and heating under ambient conditions, respectively.

Compound	Wavelength (nm)	$\tau_1$ (ms)	A <sub>1</sub> (%)	$\tau_2$ (ms)	A <sub>2</sub> (%)	$\tau_3$ (ms)	A <sub>3</sub> (%)
Grinding	396	30.25	52.94	352.55	47.06		
	445	2.54	9.85	37.26	51.76	315.82	38.39
	543	73.21	4.42	719.58	95.58	-	-
	585	647.59	100	-	-	-	-
Fuming	396	0.8	35.49	26.32	41.16	135.77	39.54
	445	1.0	12.85	31.00	50.79	238.01	36.36
	543	15.36	10.51	499.27	89.49		
	585	13.35	7.27	488.60	92.73		
Heating	396	0.31	32.29	26.73	44.27	152.20	22.44
	445	0.62	22.21	29.46	51.28	180.83	26.50
	543	1.03	40.58	18.01	16.70	314.53	42.72
	585	0.97	35.97	14.55	15.24	317.33	48.79

**Table S12** Natural Transition Orbitals (NTOs) representing the T<sub>1</sub> state energy transitions





The theoretical calculation was carried out to further confirm our speculation for TTA. As shown in Table S12, the electron clouds localized at the adjacent carbazole substituents with efficient  $\pi\ldots\pi$  stacking, indicating that the efficient  $\pi\ldots\pi$  stacking in DCzCT and DCzOT dimers is beneficial for TTA. From the single-crystal structure, there existed stronger  $\pi\ldots\pi$  stacking (3.498 Å) between two carbazole units for DCzCT than DCzOT (3.528 Å). Combining theoretical calculation and experimental results, we speculate that the efficiency of TTA follows the order of DCzCT > DCzOT > DCzNT in crystal.

#### V. Complementary videos

**SV1, SV2 and SV3.** Under incandescent, DCzOT, DCzCT and DCzNT compounds showed as whitish crystal. These materials emitted blue light when excited with a 365 nm lamp. After the lamp was turned off, a yellow ultralong phosphorescence were observed by the naked eye for all compounds. These processes were repeated for second times and the same phenomenon were observed.